Environmental Science and Ecotechnology 30 (2026) 100679

Contents lists available at ScienceDirect

Environmental Science and Ecotechnology

journal homepage: www.journals.elsevier.com/environmental-science-and-ecotechnology/

Original Research

Host metabolic integration enables superior polystyrene degradation in cockroaches

Mei-Xi Li [a,b], Yu-Qian Wang [a], Jia-Yi Wang [a], Meng-Qi Ding [a], Shan-Shan Yang [a,b,*], Jie Ding [a,b], Wei-Min Wu [c]

[a] National Engineering Research Center for Safe Disposal and Resources Recovery of Sludge, Harbin Institute of Technology, Harbin, 150090, China
[b] State Key Laboratory of Urban-rural Water Resource and Environment, School of Environment, Harbin Institute of Technology, Harbin, 150090, China
[c] Department of Civil and Environmental Engineering, William & Cloy Codiga Resource Recovery Center, Stanford University, Stanford, CA, 94305, USA

ARTICLE INFO

Article history:
Received 10 May 2025
Received in revised form
24 February 2026
Accepted 24 February 2026

Keywords:
Blaptica dubia
Polystyrene
Biodegradation
Gut microbiota
Enzymes

ABSTRACT

Plastic pollution is a global crisis, with polystyrene (PS) among the most recalcitrant polymers owing to its stable aromatic structure and resistance to natural degradation. Although insect larvae such as mealworms and wax moth caterpillars can partially biodegrade PS through gut microbiota, reported rates remain low (0.08–0.24 mg per individual per day). The potential of cockroaches—with more stable gut microbiomes, longer lifespans, and greater biomass—for efficient, scalable plastic bioremediation has remained unexplored. Here we show that *Blaptica dubia* cockroaches rapidly biodegrade PS microplastics via a tightly integrated host–microbiota enzymatic network. Individuals ingested 6.0 ± 0.2 mg PS daily, achieving 54.9 ± 2.3% mass loss over 42 days and a specific biodegradation rate of 3.3 ± 0.1 mg per cockroach per day. Biodegradation was confirmed by substantial molecular-weight reductions (Mn 46.4%, Mw 25.9%) and isotopic mineralization signatures. PS exposure selectively enriched plastic-degrading taxa and enzymes while strongly upregulating host fatty-acid β-oxidation and tricarboxylic acid cycle pathways, enabling the host to directly metabolize microbial cleavage products and reconstruct a complete PS catabolic pathway. These findings reveal that *B. dubia* can far outperform other insects in plastic biodegradation through evolved metabolic cooperation, expanding the biological repertoire for tackling persistent anthropogenic polymers and offering new insight into insect adaptation to synthetic substrates in the Anthropocene.

1. Introduction

Plastic pollution has emerged as a severe global environmental challenge, with micro- and nanoplastics detected in almost all ecosystems [1,2]. Plastic fragments exposed to ultraviolet radiation and physical abrasion are transformed into microplastics (<5 mm) and nanoplastics (<1 μm). Owing to their hydrophobic surfaces, microplastics can efficiently adsorb and concentrate hydrophobic organic contaminants and accumulate heavy metals, thereby acting as vectors of priority pollutants and posing potential risks to human health [3]. Global plastic production has reached 400.3 million tons per year, with polyethylene (PE), polypropylene (PP), and polystyrene (PS) as the major products [4]. PS accounts for 6.7% of plastics and is widely used in packaging and insulation due to its lightweight, low cost, and thermal properties [5]. Its benzene-ring backbone and stable C–C main chain render PS chemically inert and environmentally persistent, with natural degradation extremely slow—taking decades to millennia—even under the action of common environmental microbes from soil or marine systems [6]. Plastic debris accumulates in freshwater and soil systems and alters water properties, soil structure, nutrient cycles, and microbial communities [7–9]; recycling remains extremely limited due to economic and technical constraints [10]. Conventional treatments—including pyrolysis, photocatalysis, and solvent-based methods—face bottlenecks, such as high energy demand, slow kinetics, or toxic byproducts [11–14]. In contrast, biodegradation provides milder, low-pollution alternatives: environmental microbes secrete oxidases and hydrolases that promote

* Corresponding author. National Engineering Research Center for Safe Disposal and Resources Recovery of Sludge, Harbin Institute of Technology, Harbin, 150090, China.
E-mail address: shanshanyang@hit.edu.cn (S.-S. Yang).

https://doi.org/10.1016/j.ese.2026.100679

polymer chain scission, accelerate conversion into small molecules, and integrate them into complex metabolic networks and biogeochemical cycles [15–17]. Certain functional microbial taxa play key roles in carbon cycling and energy metabolism, suggesting that microplastics may undergo multistage biodegradation in natural environments [18,19]. These advances expand the understanding of plastic fate and provide theoretical foundations and technological strategies for polymer biodegradation.

An increasing number of studies have shown that insects possess unique advantages for plastic biodegradation, demonstrating clear capacities for both the initial depolymerization of plastics and their subsequent metabolic conversion [20,21]. Representative plastic-degrading insect species have been reported in the Coleoptera order, including Tenebrionidae (e.g., *Tenebrio molitor, Tenebrio obscurus, Zophobas atratus*, *Plesiophthalmus davidis*, *Uloma* sp., and *Uloides dermestoides*), Scarabaeidae (e.g., *Protaetia brevitarsis*), and in the Lepidoptera order, including Pyralidae (e.g., *Galleria mellonella*, *Achroia grisella*, *Podia interpunctella*, and *Gryllodes sigillatus*) [20,22–26]. Research on plastic degradation by insects is still in its early stages and includes only a limited number of insects [27,28]. Among these, *T. molitor* larvae are the most widely investigated plastic degraders, which ingest and biodegrade PS, PE, polyvinyl chloride (PVC), PP, polyethylene terephthalate (PET), and polyurethane (PUR), with gut microbial communities playing a key role [20,29–34]. *G. mellonella* and *Z. atratus* are also well investigated insect species for the biodegradation of PS, PP, and PE; their gut microbial diversity, host digestive enzyme activities, and antioxidant stress pathways are all closely associated with the efficiency of plastic degradation [20,31,33,35]. Overall, the plastic degradation rate caused by these insects is much higher than that of isolated gut plastic-degrading strains *in vitro*, by hundreds of times, with the half-life of plastics calculated in hours rather than weeks to months [20,27]. To date, relatively few insect species have been identified as plastic degraders or plastivores [20,23,33], and research has largely focused on Lepidoptera and Coleoptera. In general, the existing mechanistic studies are relatively fragmented and lack a systematic integration of host, microbial, and enzymatic contributions. This limitation highlights the need for multi-omics approaches to elucidate plastic-degradation mechanisms and underscores the importance of expanding investigations to additional insect models, such as *T. molitor*, *Z. atratus*, and *G. mellonella*.

Blaptica dubia (*B. dubia*) is a cockroach that belongs to the order Blattodea, which includes 4400 cockroach species and approximately 3000 termite species. *B. dubia* primarily feeds on fruits, grains, and decaying plant matter (both sexes as shown in Supplementary Fig. S1h); moreover, it shares a close evolutionary relationship with termites [36], which are well known for degrading lignin and other complex aromatic polymers, such as cellulose, hemicellulose, and humic substances. Although *B. dubia* is a frugivore, it can digest the cellulose fiber found in its plant-based diet. The ability to digest tough polymers, such as lignocellulose (wood), is linked to the potential to break down plastics, which share similar chemical structures. Because both PS and lignin contain aromatic backbones, this structural similarity—together with their evolutionary connection—suggests that *B. dubia* may possess an inherent capacity to process such aromatic polymeric substrates. Physiologically, the gut of *B. dubia* accounts for approximately 15–20% of its body mass—substantially higher than that of other commonly studied plastic-degrading insects (such as *T. molitor*)—thereby providing extensive spatial and functional capacity to support complex and diverse microbial communities [37]. This highly developed gut architecture not only facilitates stable host–microbe symbiosis but likely also enhances the processing of chemically and structurally recalcitrant macromolecules. Combined with its broad diet breadth and strong environmental adaptability [38–40], *B. dubia* emerges as a compelling model for investigating host–microbe cooperative mechanisms underlying plastic biodegradation.

To elucidate the metabolic mechanisms underlying PS biodegradation in *B. dubia*, we established an integrated analytical framework focused on plastic biodegradation, gut microbial functions, host metabolic regulation, and key enzymatic activities. The research design encompasses three complementary dimensions. First, we assessed the occurrence and chemical characteristics of biodegradation by quantifying changes in PS molecular weight, examining stable carbon isotope ($\delta^{13}C$) signatures, and characterizing pyrolysis-derived products. Second, we applied metagenomic sequencing to resolve shifts in gut microbial community composition, functional gene profiles, and microbe–enzyme interaction networks, thereby enabling the evaluation of microbial and enzymatic contributions to PS degradation. Third, we conducted transcriptomic analyses to characterize host responses across pathways of energy metabolism, redox regulation, and digestion, with the aim of identifying host metabolic processes potentially involved in PS degradation. Through this multidimensional analytical strategy, a systems-level platform was constructed to evaluate the PS-degrading potential of *B. dubia* and provide a methodological basis for investigating plastic-degrading capacities in other insect species.

2. Materials and methods

2.1. B. dubia, plastic materials, and feedstock preparation

Additive-free PS powders (particle size <100 μm) were purchased from Qianjing New Materials Co., Ltd. (Dongguan, China). They are additive-free with a weight-average molecular weight (M_w) of 283.0 kDa, number-average molecular weight (M_n) of 107.0 kDa, and Z-average molecular weight (M_z) of 548.7 kDa. We tested the feasibility of biodegrading PS MPs because they not only widely occur in environments but are also more resistant to degradation than PS foams due to their rigidity and lower surface area. Cornmeal and wheat bran were sterilized prior to feeding. Experimental *B. dubia* roaches were obtained from the Harbin Insect Breeding Facility (Harbin, China). Upon arrival, cockroaches were acclimated in a light-free, artificial insect incubator at 25–27 °C and 60–70% relative humidity. Individuals selected for the experiments were approximately 3 months old and 20–25 mm in body length. The *B. dubia* control group was fed a standard diet of carrot, apple, cornmeal, and wheat bran (6:2:1:1, w/w).

2.2. Biodegradation of PS polymer in B. dubia

To assess the feasibility of PS biodegradation, the experimental sample was divided into four groups (50 individuals per group, in triplicate): starvation, control (normal diet), PS diet, and agar groups. The PS diet was prepared by mixing PS powder with agar and deionized water (1:5:49, w/w). Specifically, agar and deionized water were heated in a water bath, cooled, and then combined with PS powder to form PS–agar gel sheets. Prior to the experiment, all *B. dubia* individuals were fasted for 24 h to eliminate potential confounding variables, such as residual gut contents from previous diets, transient dietary metabolites, and short-term diet-induced fluctuations in gut microbial communities. Body weight was measured before testing. The experimental duration was 42 days, with weekly recordings of body weight, the number of surviving insects, the amount of food provided, and food consumption. Except for the starvation group, all groups received unlimited food throughout the experiment. At the end of the trial,

clean frass (excreta) was collected from each group, dried at 50 °C for 24 h, stored in a desiccator for 12 h, and then sealed in glass tubes for subsequent analysis.

2.3. PS consumption rate and fecal characterization of B. dubia

We calculated the PS consumption rate as the mass of PS consumed per individual cockroach during the experiment (mg per cockroach). We determined the PS removal rate based on the total weight of PS consumed, the total weight of frass produced, and the residual PS content in the frass. To assess temporal trends in PS consumption, we recorded weekly PS consumption and the PS removal rate at the end of the 42-day trial. For the PS removal assay, cockroaches were provided with 3 g of diet (1 g PS, 9.8 mL water, and 0.2 g agar). Frass was collected, dried at 50 °C for 24 h, cooled in a desiccator for 12 h, and then ground into a fine powder. The powder was washed with deionized water and 75% ethanol to remove water-soluble and ethanol-extractable substances. The dried residue was extracted using tetrahydrofuran (THF) and filtered. The filtrate was left to evaporate in a fume hood, and the resulting white solid residue was weighed and regarded as residual PS to estimate the PS removal rate. For frass composition analysis, 0.1 g of clean frass from the 42-day group was dried, ground, washed with deionized water, dried again, and then weighed to determine the inorganic salt content. The remaining material was extracted with 75% ethanol to recover ethanol-soluble proteinaceous components. The dried solids were then extracted with THF and filtered to obtain the final chemical composition profile of the frass.

2.4. Characterization of residual PS polymers in B. dubia frass

2.4.1. Gel permeation chromatography analysis

We measured polymer molecular weight by gel permeation chromatography (GPC) using an Agilent GPC50 system equipped with two PLgel 10 μm MIXED-B columns and a refractive index detector. THF served as the mobile phase at 1.0 mL min^{-1}, with the column temperature maintained at 30 °C and an injection volume of 100 μL. We calibrated the system using narrow-dispersity PS standards. Samples were dissolved in THF (approximately 10 mg in 5 mL), filtered, and subjected to GPC analysis. After system stabilization, we recorded the retention times and peak molecular weights of the PS standards and calculated the molecular weight and distribution parameters of the samples using the system software [41,42]. The polydispersity index (PDI) was calculated as PDI = M_w/M_n.

2.4.2. Fourier- transform infrared spectroscopy and proton nuclear magnetic resonance analysis

Prior to testing, all samples were dried and cooled to eliminate moisture interference. For Fourier-transform infrared spectroscopy (FTIR) analysis, we prepared KBr pellets by grinding samples with potassium bromide (KBr) and pressing the mixture into transparent pellets using a tablet press [43]. We collected spectra on a Nicolet iS20 FTIR spectrometer (Thermo Fisher Scientific, USA) over 4000–400 cm^{-1} to characterize the major functional groups in the original PS and fecal samples [44]. We used proton nuclear magnetic resonance (^{1}H NMR) analysis to confirm PS oxidation and degradation [45]. Dried samples were dissolved in deuterated chloroform and transferred to NMR tubes (4–5 cm fill height; ~500–600 μL). Spectra were acquired using a Bruker 400 MHz NMR spectrometer (Germany) using the zg30 pulse sequence (400.15 MHz), with a 1.00 s relaxation delay, 4 s acquisition time, and 16 scans per sample.

2.4.3. Thermogravimetric analysis

We performed thermogravimetric analysis using a simultaneous thermal analyzer (Rigaku TG-DTA8122, Japan) to determine the thermal decomposition characteristics of PS and fecal samples. Approximately 5 mg of each sample was placed in an alumina crucible and heated to 800 °C at 20 °C min^{-1} under a high-purity nitrogen atmosphere (99.99%) at 10 mL min^{-1} until complete decomposition was achieved.

2.4.4. Stable carbon isotope analysis

We measured stable carbon isotope ratios ($\delta^{13}C$) to evaluate PS biodegradation by comparing the isotopic signatures of pristine PS and residual PS in fecal samples [46]. $\delta^{13}C$ was quantified using an elemental analyzer–isotope ratio mass spectrometer (EA-IRMS; Vario EL Cube–IsoPrime 100, Elementar, Germany). The $\delta^{13}C$ shift (‰) was calculated as:

$$\delta^{13}C = \left(\frac{R_{sample}}{R_{standard}} - 1\right) \times 1000, R = \frac{^{13}C}{^{12}C}$$

The $\delta^{13}C$ values were calibrated against the international carbon isotope standard Vienna Pee Dee Belemnite (VPDB). The overall measurement precision for $\delta^{13}C$ was ±0.10‰.

2.4.5. Pyrolysis–gas chromatography/mass spectrometry analysis

We performed pyrolysis–gas chromatography/mass spectrometry (Py-GCMS) analysis using a pyrolyzer (EGA-PY-3030D) coupled with a GC–MS system (GCMS-QP2020NX, Shimadzu, Japan) [47]. Pyrolysis was conducted at 800 °C for 0.2 min. Chromatographic separation was achieved on an HP-5MS capillary column (30 m × 0.25 mm × 0.25 μm). The injector was set to 300 °C, with high-purity helium as the carrier gas (1.0 mL min^{-1}) and a split ratio of 40:1. The oven program was specified in the following manner: initial temperature 40 °C (3 min), ramped at 10 °C min^{-1} to 140 °C, then at 20 °C min^{-1} to 310 °C (8 min). Mass spectra were acquired with an ion source temperature of 230 °C and an interface temperature 310 °C under electron impact ionization (70 eV), scanning range 29–600 *m/z* over 0–29.5 min. Samples were extracted with THF, dried, and analyzed.

2.5. Bioinformatics analysis of metagenomic sequencing

At the end of the experiment, *B. dubia* bodies were sterilized with 75% ethanol. Cockroaches were then dissected in a sterile biosafety cabinet, and intact intestinal tracts were removed and placed into sterile cryovials. Samples were snap-frozen in liquid nitrogen for 30 min and stored at −80 °C. We extracted DNA using the PF Mag-Bind Soil DNA Kit. DNA purity was measured with a NanoDrop 2000 spectrophotometer, and DNA concentration was determined using a TBS-380 fluorometer. DNA integrity was assessed by 1% agarose gel electrophoresis (5 V cm^{-1}, 20 min). DNA was then sheared into ~400 bp fragments using a Covaris M220 ultrasonicator.

We constructed libraries using the NEXTFLEX Rapid DNA-Seq Kit. The main steps included enzymatic ligation of DNA fragments with specific sequencing adapters, followed by magnetic bead-based size selection to remove adapter dimers. Libraries were then amplified by PCR with a high-fidelity DNA polymerase and purified twice with magnetic bead purification to obtain the standard library products. Then, sequencing analysis was performed on the Illumina NovaSeq platform. Library molecules were anchored to the flow cell surface via base pairing and underwent bridge amplification to form high-density DNA clusters. After linearization of the amplicons, paired-end sequencing was performed using the sequencing-by-synthesis (SBS) method. This

process employed a modified DNA polymerase and four-color fluorescently labeled dNTPs, thus enabling single-nucleotide extension cycles through reversible termination. After each cycle, fluorescence signals were captured using a laser confocal system, and the terminator groups were chemically cleaved to enable the next round of extension. Ultimately, raw sequencing data were obtained through multiple rounds of signal collection and bioinformatic analysis.

2.6. Transcriptomic analysis

Tissue samples were ground in liquid nitrogen and transferred into pre-chilled Trizol lysis buffer for thorough lysis. The lysate was centrifuged at 13,000×*g* for 5 min at 4 °C to remove impurities, and the supernatant was mixed with pre-chilled chloroform (chloroform: supernatant = 1:5, v/v) for phase separation. After centrifugation at 13,000×*g* for 15 min at 4 °C, the aqueous phase was collected and mixed with an equal volume of isopropanol to precipitate RNA. The resulting pellet was collected by centrifugation at 12,000×*g* for 10 min at 4 °C, washed twice with 75% pre-chilled ethanol, air-dried at room temperature, and dissolved in 0.1% diethyl pyrocarbonate -treated water. The total RNA was assessed for concentration (≥30 ng μL^{-1}) and purity (OD260/280 = 1.8–2.2) using a NanoDrop 2000, while integrity was evaluated via agarose gel electrophoresis and the Agilent 5300 system (RNA quality number ≥6.5). RNA samples meeting the criteria (total yield ≥1 μg) were used to construct sequencing libraries using the Illumina TruSeq™ RNA Sample Prep Kit. mRNA was enriched using Oligo dT magnetic beads, then randomly fragmented into ~300 bp segments using a fragmentation buffer. Double-stranded cDNA was synthesized using reverse transcriptase with random primers. After end repair, 3' adenylation, and ligation of Y-shaped adapters, target fragments (300 ± 50 bp) were selected using magnetic beads and enriched by PCR amplification. The libraries were quantified with a Qubit 4.0 fluorometer, followed by bridge PCR amplification on a cBot system to generate DNA clusters. Thereafter, paired-end sequencing was performed on the Illumina NovaSeq X Plus platform using the SBS technology, which involves single-base cyclic extension using four-color fluorescently labeled dNTPs and reversible termination reactions. Fluorescence signals were captured by a laser confocal imaging system and decoded through multiple sequencing cycles.

2.7. Statistical analysis

Experimental data are presented as mean ± standard deviation (SD) from three independent replicate experiments. Statistical analyses were conducted using GraphPad Prism 9 (v 9.0.0) and Origin 2021 (v 9.8.0). Differences between groups were assessed using a two-sample Student's *t*-test. $P < 0.05$ was considered statistically significant ($\alpha = 0.05$).

3. Results and discussion

3.1. PS consumption, biodegradation, and bioassimilation

We tested the biodegradation efficiency of PS in *B. dubia* cockroaches (50 individuals, $n = 3$). Over 42 days, the cockroaches ingested an average of 12.3 g of PS, corresponding to an individual consumption rate of 6.0 ± 0.2 mg per day. As the feeding period progressed, cockroaches gradually adapted to the PS diet, and the PS consumption rate progressively increased from 36.7 to 57.3 mg per individual cockroach per week (Supplementary Fig. S1a). By day 42, the average body weight of cockroaches in the PS group stabilized at 0.6 ± 0.02 g per cockroach (Supplementary Fig. S1b), which was 80.7% higher than that of the starvation group (0.3 ± 0.01 g per cockroach), but slightly lower than the agar (0.6 ± 0.02 g per cockroach) and control groups (0.7 ± 0.03 g per cockroach) (Fig. 1b). This indicates that although PS is not an ideal nutritional source, *B. dubia* can still partially utilize a PS-containing diet to sustain basic metabolic activity. Further, the results of survival rates (Fig. 1a) revealed that the PS group's survival rate (95.3 ± 3.1%) was 15.3% higher than that of the starvation group (82.7 ± 8.1%), but slightly lower than that of the control group (97.3 ± 1.2%) and agar group (96.0 ± 2.0%). Survival rate and body weight data indicate that *B. dubia* can survive to some extent on a PS-based diet, but the PS diet alone is insufficient to support its normal growth and development.

Mass balance calculations revealed that *B. dubia* removed 54.9 ± 2.3% (Supplementary Fig. S1d) of ingested PS MPs over the 42-day period ($n = 3$), thus indicating an average specific PS removal rate of 3.3 ± 0.1 mg per cockroach per day. This indicates that approximately half of the ingested PS underwent biodegradation in the insect's digestive system, potentially involving physical fragmentation, chemical oxidation, and partial mineralization.

Further, the half-life of ingested PS MPs was estimated at 27.7 ± 2.0 h based on a digestive time of 24 h that is consistent with most investigators in the extant literature. The specific PS removal rate per individual was much greater than that of mealworms (*T. molitor* larvae), which ranges from 0.08 to 0.24 mg per larva per day [30,48], likely due to the larger body size of *B. dubia* [24]. To further determine the composition of cockroach frass, a series of separation and quantification methods was applied, revealing mass proportions of 2.8%, 2.1%, 56.1%, and 39.1% for inorganic salts, proteins, residual plastic, and other substances, respectively (Supplementary Fig. S1d). These data suggest that, despite 42 days of degradation, the frass still contained a significant amount of undigested PS polymer, indicating that PS biodegradation persisted. The remaining insoluble substances that could not be dissolved in THF were classified as other impurities, which may include insoluble microbial metabolites, chitin fragments, and other unidentified organic or inorganic components. Frass excreted by *B. dubia* after feeding on PS was collected, dried, and examined using scanning electron microscopy. Compared to raw PS, the processed material exhibited an irregular, porous structure (Supplementary Fig. S2c and f). Energy-dispersive X-ray spectroscopy elemental analysis indicated that the carbon content decreased to 81.0% from 99.3% in the original PS, while the oxygen content increased from 0.7% to 18.9% (Supplementary Fig. S2g and h), thus confirming the presence of PS degradation intermediates with oxygen-containing functional groups in the frass.

3.2. Characterization of PS biodegradation

We used ^{13}C isotopic analysis to verify PS biodegradation. In the biogeochemical cycle of carbon, the lighter isotope ^{12}C is preferentially oxidized or enzymatically degraded, while the heavier isotope ^{13}C tends to be retained and excreted during metabolism. We therefore measured stable carbon isotope ratios ($\delta^{13}C$) for the pristine PS MPs and the residual PS in the excreta. The $\delta^{13}C$ value of the pristine PS sample and was −28.1 ± 0.04‰, whereas $\delta^{13}C$ for residual PS in the frass increased to −25.2 ± 0.27‰ (Fig. 1c). The increased $\delta^{13}C$ indicates that during the biodegradation process in the gut of *B. dubia*, chemical bonds containing ^{12}C were preferentially consumed, thereby leading to a relative enrichment of ^{13}C in the residual PS in the frass. This result provides a unique perspective on the PS metabolic pathway in *B. dubia* and confirms that substantial PS biodegradation occurs within the cockroach. These results are consistent with those of $\delta^{13}C$ analysis conducted

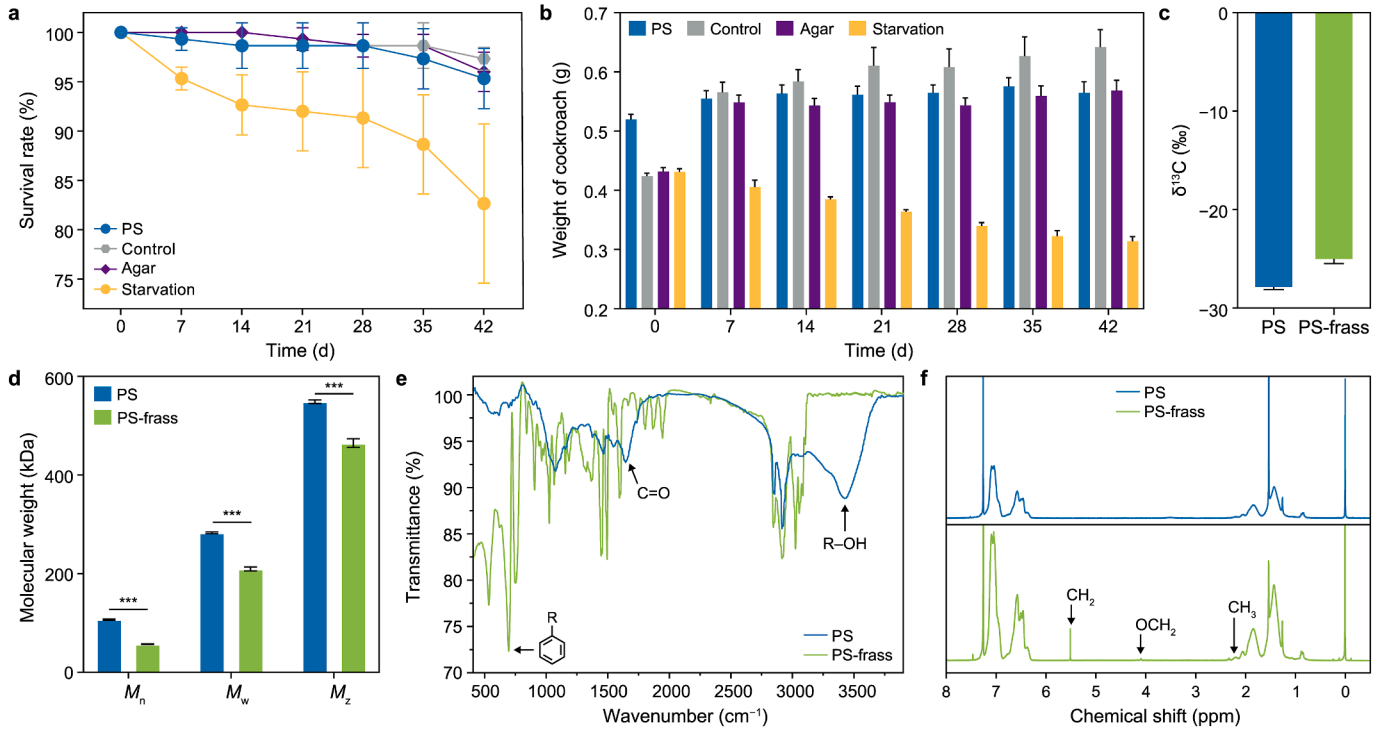

Fig. 1. Characterization of polystyrene (PS) degradation by *Blaptica dubia*. a, Survival rate of *B. dubia* in the PS-fed, standard-diet control, agar, and starvation groups. **b**, Weight changes of *B. dubia* across the same treatments. **c**, Changes in the $\delta^{13}C$ value of residual PS in the original PS and PS recovered from frass after ingestion (PS-frass). **d**, Gel permeation chromatography-derived molecular-weight metrics, including number-average molecular weight (M_n), weight-average molecular weight (M_w), and Z-average molecular weight (M_z), were measured for pristine PS and PS recovered from frass (PS-frass) at Day 42. Error bars represent mean ± standard deviation ($n = 3$). ***$P \leq 0.001$. **e**, Fourier-transform infrared spectra comparison of PS and PS-frass. **f**, Comparison of ^1H NMR spectra of PS and PS-frass.

during plastic biodegradation (PS, PE, PP, or PET) by *T.monior* [32,49–51], *Uloides dermestoides* [24], and *Protaetia brevitarsis* [23]—that is, the $\delta^{13}C$ values of residual polymers increased significantly after biodegradation, supporting that $\delta^{13}C$ analysis is an effective and reliable tool for the characterization of plastic biodegradation.

Gel permeation chromatography analysis revealed that after degradation by *B. dubia*, the number-average molecular weight (M_n) of PS in fecal samples decreased from 107.0 to 57.3 kDa, the weight-average molecular weight (M_w) decreased from 283.0 to 209.8 kDa, and the Z-average molecular weight (M_z) decreased from 548.7 to 465.0 kDa (Fig. 1d). M_n, M_w, and M_z decreased by 46.4%, 25.9%, and 15.3%, respectively, thereby revealing typical broad depolymerization pattern [20]. The analysis of the cumulative molecular-weight fraction and molecular-weight distribution revealed that the residual PS in the frass exhibited a markedly broadened distribution with a pronounced shift toward lower molecular weights, as shown by PDI increasing from 2.6 to 3.7 (Supplementary Fig. S1e and f). The reduction in molecular weight indicates that PS underwent chain scission by *B. dubia* during biodegradation at a high rate, with macromolecules being broken down into smaller oligomers [20].

Thermogravimetric (TG) analysis revealed a new decomposition peak in the fecal samples of *B. dubia*, ranging from 265 to 387 °C, with the residual mass being approximately 10% lower than that of the original sample (Supplementary Fig. S1c). This thermal instability suggests that the PS backbone structure was damaged, likely due to the cleavage of long-chain polymers into low-molecular-weight oligomers.

Fourier-transform infrared spectroscopy (FTIR) analysis revealed significant changes in the vibrational spectra: compared to the original sample, the PS surface functional groups in the fecal sample revealed alterations. The intensity of the ring-bending vibration peaks in the range 625–970 cm^{-1} decreased, while a new C=O functional group appeared around 1700 cm^{-1}, and a new –OH group was observed at 3500–3300 cm^{-1} (Fig. 1e). These findings indicate loss of PS structural features and the formation of oxygen-containing functional groups during gut-mediated biodegradation, consistent with previously reported insect-mediated degradation processes [29].

^1H NMR analysis of the original PS and PS degraded by cockroaches after 42 days revealed significant structural changes. Compared to the original PS, the PS treated by *B. dubia* exhibited new characteristic signals: a distinct OCH_2 proton peak at 4.1 parts per million (ppm) indicated the formation of ether or ester oxygen-containing functional groups during oxidation. The enhanced CH_3 proton signal at 2.21 ppm may result from methyl groups binding with oxidation products or participating in secondary metabolic reactions. The appearance of a CH_2 proton signal at 5.3 ppm is likely due to the reduction of C=C double bonds or oxidative ring-opening, which leads to the formation of methylene structures (Fig. 1f).

Py-GC/MS was employed to analyze the pyrolysis products of *B. dubia* fecal samples to further validate the degradation pathways of PS in the insect gut. The results revealed that, compared with the control group, the experimental group showed the emergence of novel alcohols, aldehydes, esters, and ethers (Supplementary Fig. S1g). This indicates that the PS backbone underwent substantial oxidative cleavage during digestion, thus generating a greater abundance of oxygenated low-molecular-weight derivatives. Notably, the emergence of these oxygen-containing functional products is highly consistent with the structural changes revealed by FTIR and NMR analyses, thus indicating that PS was oxidized via a chain-scission process in the

gut of *B. dubia*, accompanied by subsequent depolymerization that generated a variety of low-molecular-weight oxygenated derivatives. As reported previously [52], similar to PS degradation by *Plesiophthalmus davidis*—a member of the darkling beetle family—this oxidation process is likely driven by the combined actions of gut microbial activities and host enzymatic reactions. On the one hand, microbial catalysis facilitates scission of the styrene backbone; on the other hand, host enzyme systems further convert the intermediates into small oxygenated molecules, thereby reducing the polymer's chemical stability and environmental persistence.

3.3. Diversity of the gut microbiota and structural differences

Metagenomic sequencing was performed on the gut microbiota of *B. dubia* from the control and PS-fed groups to investigate trends in microbial community changes. The sequencing results revealed that the Shannon diversity index (Fig. 2a) decreased from 5.3 ± 0.2 (control group, CD42) to 4.6 ± 0.1 (experimental group, PS42), thereby indicating that 42 days of a PS-based diet may have exerted selective pressure, favored the more adaptable dominant species, and significantly reduced both species richness and evenness in the gut microbiota. This finding was further supported by an increase in the Simpson diversity index (Supplementary Fig. S3a), which rose from 0.02 in the CD42 group to 0.03 in the PS42 group. In addition, the principal component analysis (PCA) results (Fig. 2c) revealed that the PS42 and CD42 samples clustered into two distinct groups, thus indicating a significant difference in the gut microbial composition between the two sample sets. This pronounced separation suggests that PS feeding substantially reshaped the gut microbiota of *B. dubia*, leading to a systematic restructuring of the microbial community. These changes reflect the host's modulation of its gut microbiota to adapt to the metabolic demands imposed by the ingestion of an exogenous carbon source. A heatmap of sample distances based on the Bray-Curtis dissimilarity coefficient (Fig. 2b) showed greater intergroup distances than intragroup distances, further confirming the systemic impact of PS on microbial community composition. We quantified the relative contributions of deterministic versus stochastic processes in community assembly using the normalized stochasticity ratio (NST), a beta-diversity-based null-model metric. NST values above 50% indicate stochastic assembly, whereas values below 50% indicate deterministic assembly. According to the NST results

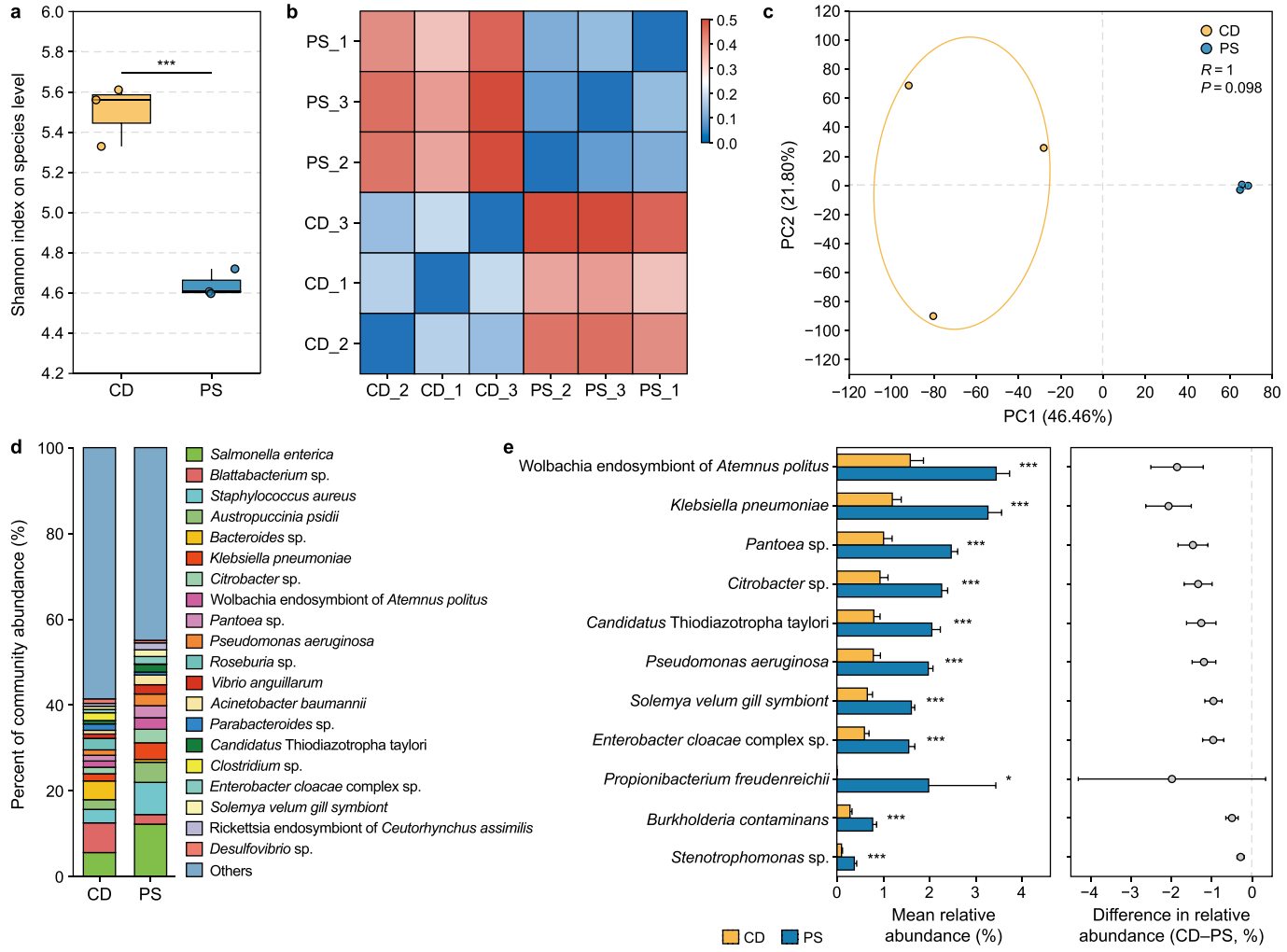

Fig. 2. Metagenomic profiling of the gut microbiome. a, Shannon diversity index. ***$P \leq 0.001$. CD: control group, *B. dubia* individuals were fed a conventional diet; PS: the experimental group fed a PS-based diet. **b**, Sample-to-sample distance heatmap. Samples labeled with _1, _2, and _3 represent three independent biological replicates for each treatment group. **c**, Principal component analysis. **d**, Species-level community composition. **e**, Differentially abundant species between the two groups (two-sided Student's *t*-test with Benjamini–Hochberg correction; adjusted $P < 0.05$, *$P \leq 0.05$, ***$P \leq 0.001$). Bars represent mean relative abundances ± standard error of the mean, and error bars in the difference plot indicate 95% confidence intervals.

(Supplementary Fig. S3b), the CD42 group had an NST of 62.9 ± 1.2%, indicating a stochastic community, whereas the PS42 group had an NST of 23.2 ± 5.0%, suggesting a deterministic community. This indicates that the PS diet induced a deterministic shift in the gut microbial community of *B. dubia*.

The Venn diagram results (Supplementary Fig. S3c) revealed that the CD42 and PS42 groups shared 8069 species, with 698 species unique to the PS42 group. Phylum-level analysis revealed that the dominant phyla in both groups were Pseudomonadota, Bacillota, and Bacteroidota, but with significant differences in their relative abundance (Supplementary Fig. S3d). In the PS42 group, Pseudomonadota accounted for 49.3%, which was markedly higher than 23.3% in the CD42 group. Bacillota constituted 13.1% and 29.6% in the PS42 and CD42 groups, respectively, while Bacteroidota decreased from 24.3% in the CD42 group to 9.9% in the PS42 group. Notably, the relative abundance of Actinobacteria—a phylum known to include strains capable of degrading aromatic compounds [53]—was higher in PS42 (4.1%) than in CD42 (1.4%), thus suggesting a potential role in PS metabolism.

Further, species-level analysis revealed that 14 species with increased abundance were enriched in the PS42 group (Fig. 2d). Among these, *Staphylococcus aureus* showed a 4.4% increase in abundance in the PS42 group compared to the CD42 group. This species, in cooperation with *Pantoea* sp.—a plastic-degrading bacterium with strong decarboxylase activity [53,54]—can jointly degrade benzene compounds [55]. The abundance of *Klebsiella pneumoniae*—which is capable of degrading vinyl compounds [56], benzoic acid, and aromatic compounds [57]—increased by 2.2%. Known PS-degrading bacteria—such as *Citrobacter* sp [58]. and *Pseudomonas aeruginosa* [59]—also revealed increased abundance. Additionally, the abundance of the symbiotic bacterium, which can oxidize alcohols into aldehydes [60], rose from 0.8% to 1.8%.

Significant difference analysis between the two groups revealed that the bacterial taxa enriched in the PS42 group exhibited remarkable performance across multiple functional categories (Fig. 2e). In addition to plastic degradation and hydrocarbon metabolism, differential microbial communities were also involved in symbiotic metabolism (e.g., *Solemya velum* gill symbiont [61]), host immune regulation (e.g., *Propionibacterium freudenreichii* produces antimicrobial peptides and activates anti-inflammatory processes [62]), and co-metabolism of pollutants (e.g., *Enterobacter cloacae* complex sp [63]. and *Burkholderia contaminans* [64]). For example, the plastic-degrading bacterium *Stenotrophomonas* sp. was significantly enriched in the PS42 group. This bacterium not only degrades compounds such as styrene but also participates in the biodegradation of unsaturated fatty acids into their derivatives [65,66].

Linear discriminant analysis effect size discriminant analysis revealed that the gut microbiota of the control group was dominated by the core taxa associated with dietary fiber and polysaccharide degradation (Supplementary Fig. S3f), such as *Bacteroides*, *Clostridium* sp., and *Ruminococcus* [67–69]. These bacteria harbor diverse glycoside hydrolases and fermentation pathways, thus enabling the efficient breakdown of complex polysaccharides and production of short-chain fatty acids, thereby supplying energy to the host and maintaining intestinal homeostasis. In contrast, plastic feeding markedly reshaped the microbial community, thus enriching taxa with broad substrate utilization capacities and the potential to transform diverse organic compounds. For example, *Salmonella enterica*, *Staphylococcus aureus*, and *Klebsiella pneumoniae* can metabolize aromatic hydrocarbons, alcohols, and fatty acids, thus suggesting a role in the further decomposition and utilization of intermediates derived from plastic degradation [56,57,70–73]. In addition, several taxa closely associated with polymer oxidation and organic compound degradation were significantly enriched. For example, *Pseudomonas aeruginosa* and *Acinetobacter baumannii* have been reported to possess substantial plastic-degrading capabilities [59,70,74–76], whereas *Citrobacter* sp. and *Pantoea* sp. exhibit strong redox metabolic potential, which may further facilitate the energy conversion of small-molecule intermediates [54,55,58,77].

Notably, the significant enrichment of *Propionibacterium freudenreichii* in the experimental group suggests that its roles in propionic acid fermentation and vitamin biosynthesis may provide nutritional compensation to the host [66,78], thereby alleviating metabolic and nutritional stress under conditions where plastic is the primary carbon source, for example, during plastic-dominated feeding conditions or in nutrient-poor environments with limited bioavailable organic carbon.

In summary, PS intake selectively enriched specific functional bacterial species and reshaped microbial interactions, transforming the gut microbiota of *B. dubia* cockroaches from a structure primarily focused on basic metabolism toward a functional community with PS-degrading capabilities.

3.4. Functional differences in gut microbiota based on metagenomic analysis

To obtain deeper insights into the functions of the gut microbiota, a multidimensional functional annotation and comparative analysis approach was employed to systematically investigate the significant functional differences between the PS42 and CD42 groups. At the clusters of orthologous groups (COGs) functional classification level (Supplementary Fig. S3e), the PS group revealed significant enrichment in two major categories: energy production and conversion (COG0843, COG1622, and COG1005), and carbohydrate transport and metabolism (COG2814). This indicates that PS intake drove shifts in the metabolic patterns of the *B. dubia* gut microbiota from conventional nutrient utilization toward efficient PS decomposition as a carbon source. This shift was achieved by enhancing pathways related to carbohydrate transport and energy metabolism, thereby providing the necessary substrates and energy for PS degradation. Further, Kyoto encyclopedia of genes and genomes (KEGG, a bioinformatics database used for genome, metabolic pathway, and functional annotation analysis) enzyme-level analysis (Supplementary Table S1) revealed that the PS42 group was significantly enriched in key enzymes, including redox-related translocases (EC 7.1.1.2), alkyl or aryl group transferases (EC 2.5.1.18), oxidoreductases acting on CH–OH groups and aldehyde groups (EC 1.1.1.216, EC 1.2.1.84), oxidases acting on paired donors with the incorporation or reduction of molecular oxygen (EC 1.14.18.2), and hydrolases acting on ester bonds (EC 3.1.26.4). The upregulation of these enzymes may facilitate the oxidative cleavage of the benzene ring and the modification of side chains during PS degradation, suggesting that the microbial community can achieve metabolic breakthroughs in degradation by regulating enzymatic activity.

The KEGG module-level analysis (Supplementary Table S2) revealed that the PS42 group had significantly increased gene abundance in modules related to Nicotinamide Adenine Dinucleotide Health (NADH) dehydrogenase (M00143), fatty acid biosynthesis (M00082, M00083), cytochrome *c* oxidase (M00154), triacylglycerol biosynthesis (M00089), β-oxidation (M00861, M00862, M00087), and fatty acid elongation (M00085). These findings are consistent with the Transporter Classification Database results (Supplementary Table S3), which also highlighted enrichment in NADH dehydrogenase and cytochrome *c* oxidase. The gut microbiota of the PS42 group exhibits pronounced enhancement of energy and lipid metabolism, thereby providing

abundant reducing power and metabolic intermediates for degradation. Unlike previous reports that primarily focus on the upregulation of individual oxidases or monooxygenases, multiple metabolic modules reveal systematic upregulation. Specifically, enhancing NADH dehydrogenase and cytochrome *c* oxidase modules significantly increases the efficiency of the electron transport chain and Adenosine Triphosphate (ATP) synthesis, thereby supplying energy for high-energy-demanding processes, such as backbone cleavage and side-chain oxidation. Concurrently, the coordinated activation of fatty acid biosynthesis, triacylglycerol synthesis, and β-oxidation modules enables the reutilization and storage of carbon chain fragments generated during degradation, thereby forming a dynamic "degradation–reuse–storage" cycle. Overall, the gut microbiota demonstrates a comprehensive adaptive strategy toward unconventional carbon sources, not merely through isolated enhancement of energy or lipid metabolism, but via an integrated "energy–material metabolism linkage," thereby highlighting its unique capacity for plastic degradation. In addition, Gene Ontology (GO) functional annotation revealed that at levels 3 (Supplementary Fig. S4) and 4 (Fig. 3a), the PS42 group showed significant upregulation of functions such as organic cyclic compound binding, heterocyclic compound binding, cellular aromatic compound metabolic process, heterocycle metabolic process, and organic cyclic compound metabolic process. This suggests that the gut microbiota in the PS42 group enhanced its capacity to bind and metabolize cyclic compounds, thereby enabling targeted adaptation to PS, a synthetic polymer containing aromatic ring structures. The benzene ring structure of molecules generates various aromatic and heterocyclic intermediates during degradation. The upregulation of these functions enables the microbial community to efficiently recognize and bind these cyclic substrates, thereby promoting their ring-opening cleavage and functional group modification by activating downstream metabolic pathways. This coordinated upregulation reveals that the gut microbiota adopts a "substrate-specific response" strategy to systematically reconstruct its metabolic network, thereby enabling *B. dubia* to efficiently metabolize and its intermediates. In summary, PS intake drives the cockroach gut microbiota to metabolically adapt to synthetic polymers through multilevel functional remodeling—upregulating key degradative and redox enzymes at the gene expression level and enhancing aromatic compound metabolic modules at the pathway level.

3.5. Microbe-enzyme ecological Co-occurrence network analysis

To further investigate the internal interactions of the gut microbiota and their adaptive mechanisms toward PS, we performed ecological co-occurrence network analysis. We constructed an unifactorial Spearman correlation network using the top 20 most abundant species (species-level profiles; $P < 0.05$). The results revealed that the CD42 group comprised 20 nodes and 98 edges, with 72.5% positive correlations, whereas the PS42 group contained 20 nodes and 78 edges, with 75.7% positive correlations (Fig. 3b), thus indicating that high-abundance species in both groups predominantly exhibited positive (cooperative) interactions. Notably, although the overall positive correlation pattern remained unchanged, PS feeding led to a clear shift in the core functional network of the gut microbial community: the CD42 network was centered on polysaccharide-degrading and fermentative taxa, whereas the PS42 network was dominated by species with broad carbon utilization capabilities and the potential for organic compound degradation, thereby forming a stable cooperative community adapted to the metabolism of the xenobiotic carbon source—PS. Modular analysis further revealed that the PS42 network could be divided into three functional modules. The first module was centered on the symbiont *Candidatus* Thiodiazotropha taylori [60], which served as the core hub and exhibited strong positive correlations with *Enterobacter cloacae* complex sp. [63], *Klebsiella pneumoniae* [56], and *Burkholderia contaminans* [64]. These species were primarily associated with "vinyl- and aromatic compound degradation" and "symbiotic metabolism," thus suggesting that this module may coordinate metabolic interactions to activate surrounding microbes, collectively contributing to PS degradation and symbiotic metabolic regulation. The second module was dominated by *Pantoea* sp. [54,55,79], with strong decarboxylase activity, and by *Citrobacter* sp. [58], focusing on carbon-chain cleavage and PS degradation intermediates. The third module, centered on the symbiont *Solemya velum* gill symbiont [61], primarily facilitated symbiotic metabolism and, thus, provided energy and material support to maintain the stability of the host–microbiota system. This finding is consistent with previous studies on *T. molitor*, in which a plastic-based diet induced significant restructuring of the gut microbiota, accompanied by pronounced positive interactions among microbial taxa and enhanced functions related to nitrogen fixation and organic carbon degradation [32,51,80]. The enrichment of these metabolic functions further supports the notion that the microbial community cooperatively utilizes xenobiotic carbon sources, thereby suggesting that the gut microbiota of *B. dubia* may similarly reinforce cooperative networks upon PS ingestion, thereby improving plastic degradation and host adaptability. Moreover, the modular division of labor and collaborative network patterns in the PS42 group enable the efficient integration of polymer degradation and symbiotic metabolism, thus facilitating both stable PS decomposition and the maintenance of ecological homeostasis.

The species–enzyme bifactorial correlation network further elucidated the molecular basis of microbial metabolic functions by integrating species-level microbial abundance with key enzyme correlations in the PS42 group. The network comprised 30 nodes (20 microbial species and 10 key enzymes) and 89 edges, with 69.7% positive correlations (Fig. 3c), thereby indicating that functional associations between microbes and enzymes in the PS group are predominantly synergistic. Among the identified key enzymes, EC 2.5.1.18 (transferase, transferring alkyl or aryl groups) and EC 7.1.1.2 (NADH: quinone oxidoreductase) exhibited strong positive correlations with *Candidatus* Thiodiazotropha taylori (a symbiotic bacterium) and *Citrobacter* sp. (a PS-degrading bacterium). These enzymes can catalyze alkyl side-chain transfer reactions during PS degradation, thereby facilitating exposure of the aromatic ring for subsequent oxidation while maintaining electron transport chain activity. EC 1.2.1.84 (oxidoreductase acting on aldehyde or oxo groups of donors) and EC 1.14.18.2 (oxidoreductase acting on paired donors with the incorporation of molecular oxygen) exhibited significant positive correlations with *Pantoea* sp. (benzene- and plastic-degrading bacterium) and *Klebsiella pneumoniae* (vinyl-degrading bacterium), thus suggesting that these strains likely participate in the initial hydroxylation of PS main and side chains via enzyme activity regulation. Meanwhile, EC 1.1.1.216 (oxidoreductase acting on CH–OH groups) was positively correlated with *Stenotrophomonas* sp. (aromatic compound-degrading bacterium), and EC 3.1.26.4 (ester bond hydrolase) was positively correlated with *Pseudomonas aeruginosa* (PS-degrading bacterium); this indicates that these enzymes likely act synergistically to further oxidize PS degradation intermediates into small-molecule metabolites. In addition, EC 7.6.2.4 (ATP phosphohydrolase) was closely associated with *Austropuccinia psidii*, thus suggesting that this organism may provide energy for the overall metabolic network via ATP hydrolysis. This collaborative

microbe–enzyme system is highly consistent with observations in other plastic-degrading insects, such as *T. molitor* [80], and also observed in other and plastic-feeding insects. For example, in the Black soldier fly (BSF) larvae do not reliably biodegrade common plastics (PE, PS,PP, PET PVC ec.) but plastic feeding has been shown to significantly increase the abundance of alkane hydroxylases, monooxygenases, multicopper oxidases, and laccases in the gut microbiome, highlighting the pivotal role of oxidases in the initial oxidation of aromatic rings [81]. Similarly, in *T. molitor*, PS feeding induced gut community remodeling and enrichment of fatty acid degradation, aromatic compound metabolism, and multiple oxidoreductase genes [82]. This cross-species evidence further supports the "microbe–enzyme–host" synergistic degradation model, thus suggesting that the gut microbiota of *B. dubia* may reinforce collaborative networks upon PS ingestion, thereby enhancing the degradation of exogenous carbon sources. Further, both unifactorial and bifactorial network analyses, from complementary perspectives, revealed the ecological interactions and metabolic regulatory mechanisms of the PS42 gut microbiome. The community forms a tightly connected network centered on degradative bacteria and achieves functional integration through modular organization; key species including *Citrobacter* sp., *Klebsiella pneumoniae*, *Pantoea* sp., and *Stenotrophomonas* sp., specifically regulate the activity of alkyl transferases, oxidoreductases, and other functional enzymes, thus establishing a "microbe–enzyme–substrate" coordinated response system.

3.6. Transcriptomic analysis

Transcriptomic sequencing was employed to deeply investigate gene expression differences between the PS42 treatment group and the CD42 control group. The upregulation and downregulation were induced by gut microbiota, host, or both. PCA revealed a clear separation between the PS42 and CD42 samples along PC1 and PC2 (Supplementary Fig. S5a), thus indicating that the PS diet significantly altered the transcriptome of the *B. dubia* host. The volcano plot further visualized the distribution of differentially expressed genes (Fig. 4a), with 7242 significantly different genes identified—6036 upregulated and 1206 downregulated (Supplementary Fig. S5b)—thus suggesting that under PS stress, *B. dubia* activates specific gene expression programs to cope with environmental pressure. Further, EggNOG functional annotation of the upregulated gene set revealed significant enrichment in functions related to metabolism and protein regulation. Notably, 170 and 169 genes were categorized under "Carbohydrate transport and metabolism" and "Energy production and conversion," respectively (Fig. 4b), thus indicating that PS, as a carbon source, triggered metabolic remodeling. It is also worth noting that 420 genes were enriched in the category "Translation, ribosomal structure, and biogenesis," suggesting that the upregulation of these genes may enable the maintenance of the appropriate activity of key metabolic enzymes and functional proteins by regulating protein folding, modification, and degradation.

GO level-3 functional annotation analysis revealed significant upregulation in categories such as "transferase activity," "carbohydrate derivative binding," "hydrolase activity," "heterocyclic compound binding," "small molecule binding," and "organic cyclic compound binding" (Supplementary Fig. S5c), thus suggesting that *B. dubia* under PS stress enhanced their capacity for catalyzing, binding, and metabolizing complex compounds. Further analysis at the GO level 4 revealed a similar trend, with notable upregulation in functions such as "organic cyclic compound metabolic process," "cellular macromolecule metabolic process," "cellular nitrogen compound metabolic process," "macromolecule metabolic process," "organic nitrogen compound metabolic process," and "ATP binding" (Fig. 4d). These results are highly consistent with the characteristics of PS as a high-molecular-weight polymer containing benzene rings. The activation of the "organic cyclic compound metabolic process" indicates that the host has specifically enhanced its metabolic capacity to degrade the benzene ring structure of PS. Additionally, the upregulation of the "cellular macromolecule metabolic process" and the "organic nitrogen compound metabolic process" may likely be involved in the reutilization of PS degradation intermediates and integration of nitrogen sources.

The GO functional enrichment bubble chart visually illustrates the enrichment characteristics of differentially expressed genes across biological processes, molecular functions, and cellular components. The results reveal that, in addition to "organic nitrogen compound metabolic process" and "small molecule metabolic process," we observed significant enrichment of "oxoacid metabolic process," "carbohydrate derivative binding," "organic acid metabolic process," and "carboxylic acid metabolic process" (Fig. 4c). The prominent enrichment of the "oxoacid metabolic process" suggests that organisms likely convert intermediates produced during PS degradation into oxoacid compounds via oxidation reactions, thus enabling further integration into the tricarboxylic acid (TCA) cycle.

The activation of the "organic acid metabolic process" and "carboxylic acid metabolic process" indicates that the host can effectively incorporate organic acids produced from PS degradation into its metabolic network, enabling carbon source reutilization via pathways such as β-oxidation. Based on iPath pathway analysis, pathways related to carbohydrate metabolism, energy metabolism, β-oxidation, and the TCA cycle were significantly enriched (Supplementary Fig. S6), thereby indicating that *B. dubia* systematically remodels its core metabolic network under PS stress.

The results of transcriptomic analysis revealed that, under PS stress, the gut of *B. dubia* exhibited a more complex metabolic reprogramming compared with.

The results of transcriptomic analysis revealed that under PS stress, the gut of *B. dubia* exhibited a more complex metabolic reprogramming compared with the *T. molitor*. This remodeling encompassed not only the recognition of aromatic structures, energy supply, and reintegration of degradation intermediates but also the marked upregulation of functional categories—such as "organic cyclic compound metabolism," "nitrogen metabolism," and "ATP binding"—accompanied by coordinated coupling across multiple metabolic modules. At the same time, both energy metabolism and intermediate reutilization pathways were reinforced, thereby highlighting the pivotal roles of nitrogen fixation and nitrogen cycling in *B. dubia* when consuming a carbon-rich but nitrogen-deficient plastic diet.

3.7. Proposed mechanism of PS degradation mediated by gut microbiota and host interaction

Plastic degradation requires the enzyme-catalyzed depolymerization of polymers and metabolism of degraded intermediates [28]. Based on the above results and discussion, we proposed that the overall metabolic mechanism of PS biodegradation via microbe-host enzymatic interaction in the gut of *B. dubia* drives PS degradation in the PS42 group, based on the integration of metagenomic, transcriptomic, and microbe-enzyme interaction network analyses (Fig. 5). *Candidatus* Thiodiazotropha taylori and *Citrobacter* sp. likely participate in the oxidative cleavage of the PS backbone by secreting EC 2.5.1.18 (alkyl/aryl transferase) and EC 7.1.1.2 (NADH: quinone oxidoreductase), thereby fragmenting the polymeric carbon skeleton into shorter

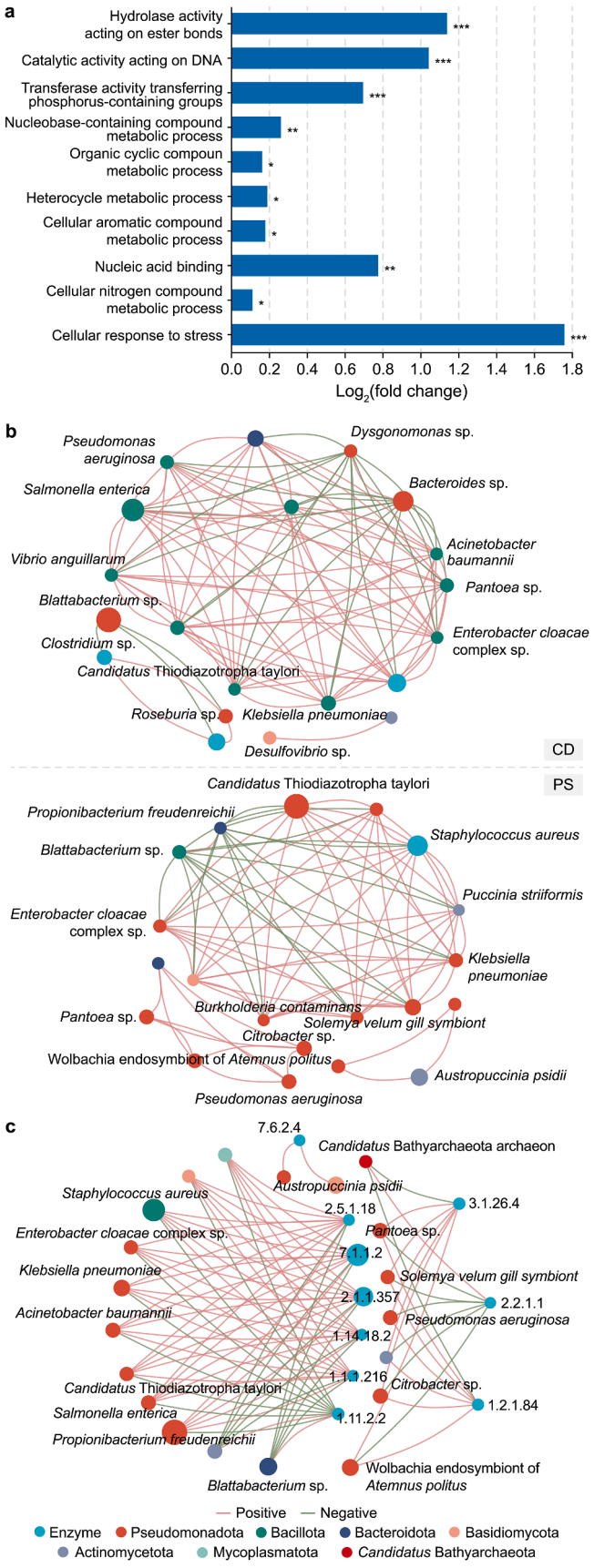

Fig. 3. Functional shifts and co-occurrence networks of the gut microbiome. a, Fold change in Gene Ontology (GO) level 4 functional categories between groups (two-sided Student's *t*-test with Benjamini–Hochberg correction; adjusted $P < 0.05$, $^{*}P \leq 0.05$, $^{**}P \leq 0.01$, $^{***}P \leq 0.001$). **b**, Univariate co-occurrence network of the 20 most abundant species inferred using Spearman correlations ($|\rho| \geq 0.5$; $P < 0.05$) in the control (CD) and polystyrene (PS) group. **c**, Bifactorial network analysis integrating the 20 most abundant species and 10 key enzymes. Node color denotes phylum, and edges indicate positive or negative associations. Node size represents species or enzyme abundance, with larger nodes indicating higher abundance.

chains. *Pseudomonas aeruginosa* likely secretes EC 3.1.26.4 (ester bond hydrolase) to act on aromatic side chains, thus initiating the opening of benzene rings and triggering the aromatic degradation pathway. Moreover, PS may generate styrene monomers via radical scission [83,84]. These styrene intermediates are further oxidized by *Pantoea* sp. and *Klebsiella pneumoniae* through EC 1.2.1.84 (aldehyde/oxygen oxidoreductase) and EC 1.14.18.2 (oxidoreductase acting on paired donors with incorporation of molecular oxygen). *Stenotrophomonas* sp., via EC 1.1.1.216 (CH–OH group oxidoreductase), likely also accelerates this oxidative cleavage process. This process has been reported in multiple studies on PS biodegradation. For example, in the degradation of PS by *G. mellonella*, styrene structures were shown to be oxidized to produce phenolic and carbonyl intermediates, thus indicating the involvement of relevant oxidoreductases [85]. Similarly, studies on *T. molitor* have demonstrated that benzene rings can undergo auto-oxidation within the digestive tract, involving side-chain opening of styrene and subsequent oxidation [21,31,80,86]. Moreover, based on environmental microbial genomic data, certain researchers have predicted that P450 monooxygenases, aromatic ring dioxygenases, and other oxidoreductases could catalyze the oxidation of styrene into oxidized molecules. such as phenolic acids and benzoic acid, which then enter central metabolic pathways [87]. Notably, the synergistic interaction between *Austropuccinia psidii* and EC 7.6.2.4 (ATP phosphohydrolase) may provide the energetic drive required to sustain the entire metabolic network, thereby ensuring the continuous progression of PS degradation. Meanwhile, the small-molecule intermediates generated by gut microbes during PS degradation can be transported into host cells via transmembrane transporters, where they activate core metabolic pathways such as β-oxidation and the TCA cycle. Through oxidative phosphorylation, these intermediates enable efficient ATP synthesis, thereby establishing a "microbial degradation–host metabolism" synergistic cascade.

4. Environmental implications and future studies

The improper disposal of plastic waste has become a global environmental and ecological concern. In natural environments, the degradation of plastics not only releases toxic substances, such as persistent organic pollutants and heavy metals, but also forms microplastics and nanoplastics through fragmentation. These particles can be transferred through the food chain, thus posing widespread risks to biological systems.

Over tens of millions of years of natural evolution, ancient members of the Blattodea order—cockroaches—have developed a digestive system that is highly adapted to diverse carbon sources and complex organic substrates. This study revealed that under the current environmental pressure of escalating plastic pollution, the gut microbiota of cockroaches exhibits remarkable "xenocarbon adaptability," which is capable of utilizing synthetic polymers—such as PS—as potential carbon sources. This study reveals the biodegradation mechanism of PS by *B. dubia* and its associated microbe–host enzymatic interaction network. Through integrated metagenomic and transcriptomic analyses, it was confirmed that a multilayered metabolic collaboration exists between the cockroach's gut microbiota and host cells during PS degradation. The microbial community initiates extracellular oxidative breakdown

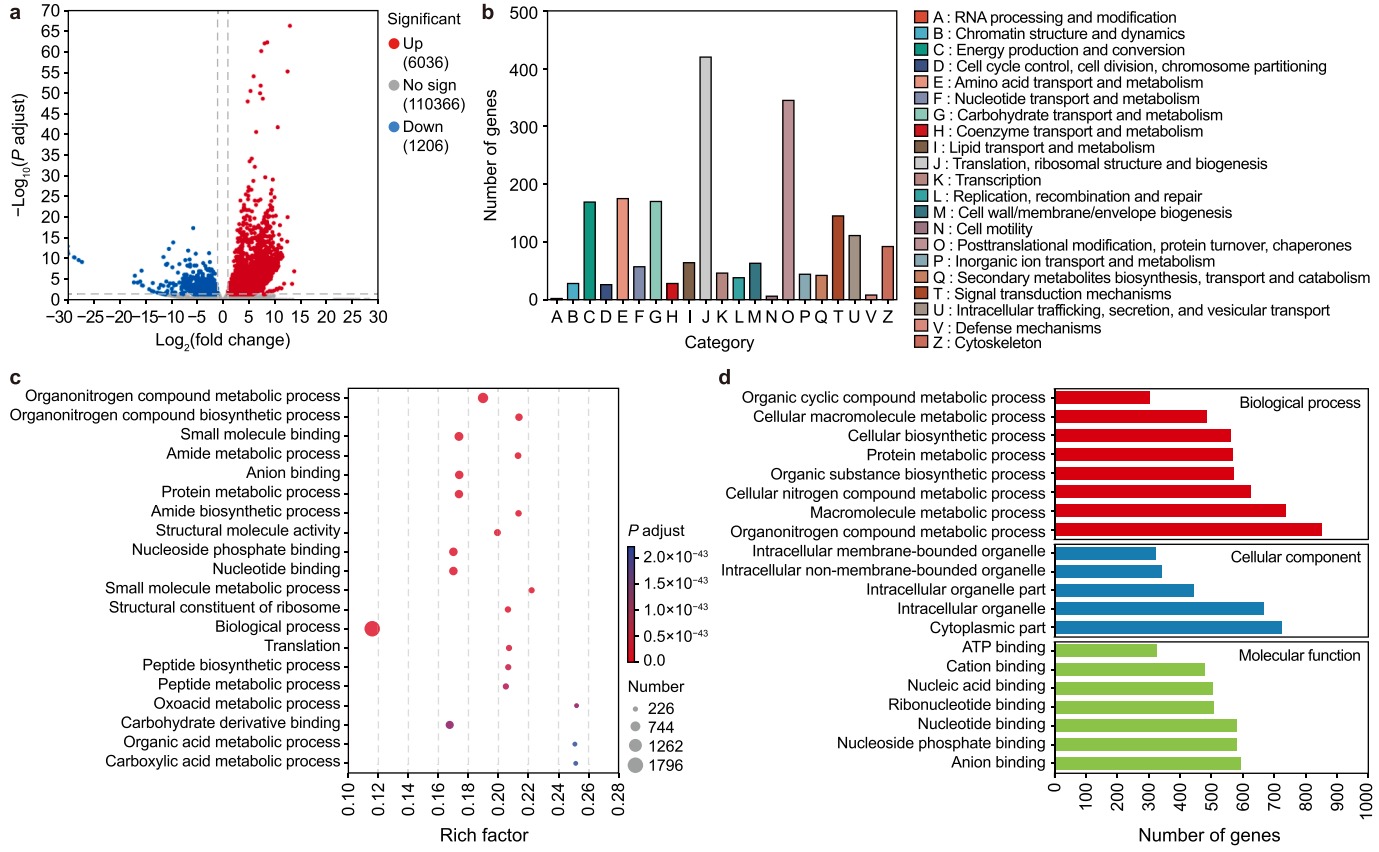

Fig. 4. Transcriptomic responses to polystyrene (PS) feeding. a, Volcano plot of differential gene expression. Genes are classified as upregulated (Up), non-significant (No sign), or downregulated (Down). The vertical dashed lines indicate the fold change thresholds, whereas the horizontal dashed line indicates the threshold for statistical significance. **b**, EggNOG functional classification bar chart of significantly upregulated genes in the PS42 group. **c**, Gene Ontology (GO) enrichment analysis. **d**, GO level 4 functional classification of the differentially expressed gene set. ATP, adenosine triphosphate.

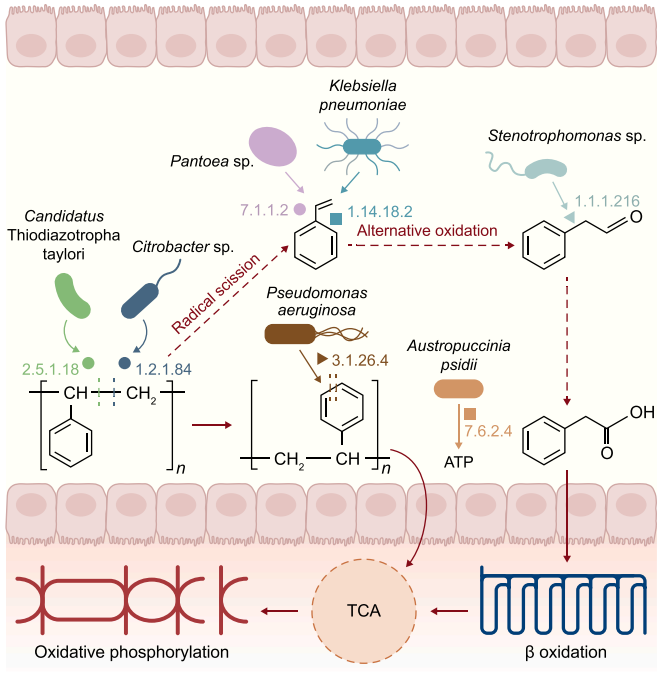

Fig. 5. Proposed mechanism of polystyrene degradation under the microbe–host enzymatic interaction system in *Blaptica dubia*. ATP, adenosine triphosphate; TCA, tricarboxylic acid cycle; β-oxidation, fatty acid β-oxidation pathway.

of PS by enriching specific degradative bacteria and functional enzyme systems. The resulting small-molecule metabolites are subsequently absorbed by host cells and processed through β-oxidation, the TCA cycle, and other pathways for efficient carbon reutilization. Ultimately, this leads to the formation of a synergistic cascade model of "microbial degradation–host metabolism." This discovery provides a novel direction for the development of sustainable biodegradation technologies for petroleum-based plastics and significantly expands existing understanding of the molecular mechanisms underlying insect-mediated plastic degradation.

In the present study, *B. dubia* was tested only for PS biodegradation. Further research will be conducted to investigate other major plastics (PE, PP, PVC, PET, PUR, etc.) to determine whether *B. dubia* possesses broad plastic-degrading ability, which is likely based on microbiome and transcriptomic analyses. *B. dubia* cockroaches are not wood-feeding cockroach species, and it remains unclear whether their plastic-degrading capacity is comparable to that of specific wood-boring cockroaches in the cockroach family, such as *Panesthia angustipennis* and *Salganea taiwanensis* [48]. The American cockroach (*Periplaneta americana*) and German cockroach (*Blattella germanica*) belong to the omnivorous feeding group and naturally consume a wide variety of plant and animal matter as well as plastic debris [88,89]. Further investigations should explore plastic degradation across different cockroach species.

Although *B. dubia* exhibits excellent PS-degrading capacity under laboratory conditions, the direct release of *B. dubia* and other cockroaches into natural environments for biodegradation

applications remains questionable, and more research is needed in this area. A comprehensive analysis and evaluation of multiple impacts—such as environmental effects, potential health risks, and public acceptance—associated with the potential release or application of *B. dubia* in natural or semi-natural environments should be conducted.

5. Conclusion

B. dubia is a newly identified plastic-degrading cockroach species in the order Blattodea and exhibits a specific PS degradation rate of 3.3 ± 0.1 mg per cockroach per day and a PS half-life of 27.7 ± 2.0 h on the basis of a digestive time of 24 h. Biodegradation is strongly supported by broad depolymerization, increases in $\delta^{13}C$ values, and the formation of various oxidized intermediate products.

Metagenomic sequencing analysis provides evidence of the shift in gut microbes to adapt to PS feeding during *in vivo* biodegradation. PS intake remodels the gut microbial community, thus enabling the coordinated enrichment of key plastic-degrading microbes and their functional enzymes, while host β-oxidation and TCA cycle pathways are significantly upregulated. This establishes a tightly coupled system, jointly driven by microbes, enzymes, and host metabolism, that continuously facilitates polymer chain cleavage and the downstream degradation of intermediate products.

Compared with single microbial strains or isolated enzyme systems, the higher degradation efficiency of *B. dubia* arises from the functional integration and systemic plastic-degrading strategy conferred by the tripartite host–microbe–enzyme collaboration, thus surpassing the limitations of conventional microbial or enzyme-based degradation and highlighting the evolutionary potential of insects to process aromatic polymer PS.

However, this study has several limitations and further research is needed. While metagenomic and transcriptomic sequencing can reveal the types and potential functions of plastic-degrading enzymes, they are insufficient to fully resolve the specific enzymatic reactions and degradation mechanisms involved. Moreover, the intermediate products and their structures formed during plastic degradation in *B. dubia* were not systematically identified or characterized in this study. To address these limitations, future research should integrate metabolomic analyses, gene cloning, enzymatic characterization, and dynamic tracing approaches to systematically explore cooperative host–microbe degradation processes, thereby providing a more comprehensive understanding of the underlying mechanisms and enabling a more robust comparison of plastic degradation ability with other cockroach species.

CRediT authorship contribution statement

Mei-Xi Li: Writing – original draft, Visualization, Validation, Methodology, Investigation. **Yu-Qian Wang:** Formal analysis. **Jia-Yi Wang:** Writing – review & editing. **Meng-Qi Ding:** Writing – review & editing, Formal analysis. **Shan-Shan Yang:** Writing – review & editing, Funding acquisition, Conceptualization. **Jie Ding:** Resources, Project administration, Funding acquisition. **Wei-Min Wu:** Formal analysis, Conceptualization.

Data availability

The raw metagenomic and transcriptomic datasets used in this study are provided in the Supplementary Information.

Declaration of competing interest

The authors declare that they have no known competing financial interests or personal relationships that could have appeared to influence the work reported in this paper.

Dr. Shan-Shan Yang, an Editorial Board Member of *Environmental Science and Ecotechnology*, was not involved in the editorial review or the decision to publish this article.

Acknowledgments

The authors gratefully acknowledge the Science Foundation of the National Engineering Research Center for Safe Disposal and Resources Recovery of Sludge (Harbin Institute of Technology) (No. K2024A007), the National Natural Science Foundation of China (Grant No. 52170131), and the State Key Laboratory of Urban-rural Water Resource and Environment (Harbin Institute of Technology) (No. 2025TS44).

Appendix A. Supplementary data

Supplementary data to this article can be found online at https://doi.org/10.1016/j.ese.2026.100679.

References

[1] C.M. Rochman, The complex mixture, fate and toxicity of chemicals associated with plastic debris in the marine environment, in: M. Bergmann, L. Gutow, M. Klages (Eds.), Mar. Anthropog. Litter, Springer International Publishing, Cham, 2015, pp. 117–140, https://doi.org/10.1007/978-3-319-16510-3_5.
[2] N. Evangeliou, H. Grythe, Z. Klimont, C. Heyes, S. Eckhardt, S. Lopez-Aparicio, A. Stohl, Atmospheric transport is a major pathway of microplastics to remote regions, Nat. Commun. 11 (2020) 3381, https://doi.org/10.1038/s41467-020-17201-9.
[3] M.A. Browne, P. Crump, S.J. Niven, E. Teuten, A. Tonkin, T. Galloway, R. Thompson, Accumulation of microplastic on shorelines woldwide: sources and sinks, Environ. Sci. Technol. 45 (2011) 9175–9179, https://doi.org/10.1021/es201811s.
[4] Plastics Europe, Plastics – the Fast Facts 2023, 2023.
[5] United Nations Environment Programme (UNEP), From Pollution to Solution: a Global Assessment of Marine Litter and Plastic Pollution, UNEP, Nairobi, 2021.
[6] H. Inderthal, S.L. Tai, S.T.L. Harrison, Non-hydrolyzable plastics – an interdisciplinary look at plastic bio-oxidation, Trends Biotechnol. 39 (2021) 12–23, https://doi.org/10.1016/j.tibtech.2020.05.004.
[7] S. Cook, S. Abolfathi, N.I. Gilbert, Goals and approaches in the use of citizen science for exploring plastic pollution in freshwater ecosystems: a review, Freshw. Sci. 40 (2021) 567–579, https://doi.org/10.1086/717227.
[8] M. Guo, S.A.F. Bon, S. Abolfathi, Transport dynamics of microplastics within aquatic vegetation featuring realistic plant morphology, Water Res. 282 (2025) 123534, https://doi.org/10.1016/j.watres.2025.123534.
[9] J. Cui, H. Tian, Y. Qi, X. Hu, S. Li, W. Zhang, Z. Wei, M. Zhang, Z. Liu, S. Abolfathi, Impact of microplastic residues from polyurethane films on crop growth: unraveling insights through transcriptomics and metabolomics analysis, Ecotoxicol. Environ. Saf. 283 (2024) 116826, https://doi.org/10.1016/j.ecoenv.2024.116826.
[10] Z. Xu, D. Sun, J. Xu, R. Yang, J.D. Russell, G. Liu, Progress and challenges in polystyrene recycling and upcycling, ChemSusChem (2024) e202400474, https://doi.org/10.1002/cssc.202400474.
[11] EPA, Toxicological Review of Tetrahydrofuran, U.S. Environmental Protection Agency, Washington, DC, 2012.
[12] T. Faravelli, M. Pinciroli, F. Pisano, G. Bozzano, M. Dente, E. Ranzi, Thermal degradation of polystyrene, J. Anal. Appl. Pyrolysis 60 (2001) 103–121, https://doi.org/10.1016/S0165-2370(00)00159-5.
[13] S. Jiang, Y. Chen, Y. Huang, P. Hu, Photooxidation of polystyrene into high-value chemicals, Eur. J. Org. Chem. 28 (2025) e202401109, https://doi.org/10.1002/ejoc.202401109.
[14] Y. Xu, Q. Ou, J.P. Van Der Hoek, G. Liu, K.M. Lompe, Photo-oxidation of micro- and nanoplastics: physical, chemical, and biological effects in environments, Environ. Sci. Technol. 58 (2024) 991–1009, https://doi.org/10.1021/acs.est.3c07035.
[15] W. Gao, M. Xu, W. Zhao, X. Yang, F. Xin, W. Dong, H. Jia, X. Wu, Microbial degradation of (micro)plastics: mechanisms, enhancements, and future directions, Fermentation 10 (2024) 441, https://doi.org/10.3390/fermentation10090441.
[16] R.S. Ridley, R.E. Conrad, B.G. Lindner, S. Woo, K.T. Konstantinidis, Potential

routes of plastics biotransformation involving novel plastizymes revealed by global multi-omic analysis of plastic associated microbes, Sci. Rep. 14 (2024) 8798, https://doi.org/10.1038/s41598-024-59279-x.
[17] J. Choi, H. Kim, Y.-R. Ahn, M. Kim, S. Yu, N. Kim, S.Y. Lim, J.-A. Park, S.-J. Ha, K.S. Lim, H.-O. Kim, Recent advances in microbial and enzymatic engineering for the biodegradation of micro- and nanoplastics, RSC Adv. 14 (2024) 9943–9966, https://doi.org/10.1039/D4RA00844H.
[18] H. Tian, Y. Du, X. Luo, J. Dong, S. Chen, X. Hu, M. Zhang, Z. Liu, S. Abolfathi, Understanding visible light and microbe-driven degradation mechanisms of polyurethane plastics: pathways, property changes, and product analysis, Water Res. 259 (2024) 121856, https://doi.org/10.1016/j.watres.2024.121856.
[19] H. Tian, L. Wang, X. Zhu, M. Zhang, L. Li, Z. Liu, S. Abolfathi, Biodegradation of microplastics derived from controlled release fertilizer coating: selective microbial colonization and metabolism in plastisphere, Sci. Total Environ. 920 (2024) 170978, https://doi.org/10.1016/j.scitotenv.2024.170978.
[20] S.-S. Yang, W.-M. Wu, F. Bertocchini, M.E. Benbow, S.P. Devipriya, H.J. Cha, B.-Y. Peng, M.-Q. Ding, L. He, M.-X. Li, C.-H. Cui, S.-N. Shi, H.-J. Sun, J.-W. Pang, D. He, Y. Zhang, J. Yang, D. Hou, D.-F. Xing, N.-Q. Ren, J. Ding, C.S. Criddle, Radical innovation breakthroughs of biodegradation of plastics by insects: history, present and future perspectives, Front. Environ. Sci. Eng. 18 (2024) 78, https://doi.org/10.1007/s11783-024-1838-x.
[21] M.-Q. Ding, J. Ding, S.-S. Yang, X.-R. Ren, S.-N. Shi, L.-Y. Zhang, D.-F. Xing, N.-Q. Ren, W.-M. Wu, Effects of plastic aging on biodegradation of polystyrene by *Tenebrio molitor* larvae: insights into gut microbiome and bacterial metabolism, Sci. Total Environ. 953 (2024) 176130, https://doi.org/10.1016/j.scitotenv.2024.176130.
[22] M.W. Ritchie, A. Cheslock, M.P.T. Bourdages, B.M. Hamilton, J.F. Provencher, J.E. Allison, H.A. MacMillan, Quantifying microplastic ingestion, degradation and excretion in insects using fluorescent plastics, Conserv. Physiol. 11 (2023), https://doi.org/10.1093/conphys/coad052 coad052.
[23] J. Jiang, Y. Liu, Q. Hu, Q. Yan, J. Zhuang, X. Cao, W.-M. Wu, D. He, Soil fauna *Protaetia brevitarsis* mediated polyethylene microplastic biodegradation, Sci. Total Environ. 999 (2025) 180340, https://doi.org/10.1016/j.scitotenv.2025.180340.
[24] Y. Dou, H. Jia, J. Wang, B. Nie, C.S. Criddle, M.E. Benbow, L. Wang, W.-M. Wu, Z. Duan, A new Coleoptera member (*Ulomoides dermestoides*) to biodegrade plastics, Environ. Sci. Technol. 59 (2025) 23739–23750, https://doi.org/10.1021/acs.est.5c08785.
[25] H. Kundungal, M. Gangarapu, S. Sarangapani, A. Patchaiyappan, S.P. Devipriya, Efficient biodegradation of polyethylene (HDPE) waste by the plastic-eating lesser waxworm (*Achroia grisella*), Environ. Sci. Pollut. Res. 26 (2019) 18509–18519, https://doi.org/10.1007/s11356-019-05038-9.
[26] H. Kundungal, K. Synshiang, S.P. Devipriya, Biodegradation of polystyrene wastes by a newly reported honey bee pest *Uloma* sp. larvae: an insight to the ability of polystyrene-fed larvae to complete its life cycle, Environ. Chall. 4 (2021) 100083, https://doi.org/10.1016/j.envc.2021.100083.
[27] S.-S. Yang, W.-M. Wu, J.-W. Pang, L. He, M.-Q. Ding, M.-X. Li, Y.-L. Zhao, H.-J. Sun, D.-F. Xing, N.-Q. Ren, J. Yang, C.S. Criddle, J. Ding, Bibliometric analysis of publications on biodegradation of plastics: explosively emerging research over 70 years, J. Clean. Prod. 428 (2023) 139423, https://doi.org/10.1016/j.jclepro.2023.139423.
[28] V. Tournier, S. Duquesne, F. Guillamot, H. Cramail, D. Taton, A. Marty, I. André, Enzymes' power for plastics degradation, Chem. Rev. 123 (2023) 5612–5701, https://doi.org/10.1021/acs.chemrev.2c00644.
[29] Y. Yang, J. Yang, W.-M. Wu, J. Zhao, Y. Song, L. Gao, R. Yang, L. Jiang, Biodegradation and mineralization of polystyrene by plastic-eating mealworms: part 2. Role of gut microorganisms, Environ. Sci. Technol. 49 (2015) 12087–12093, https://doi.org/10.1021/acs.est.5b02663.
[30] Y. Yang, J. Yang, W.-M. Wu, J. Zhao, Y. Song, L. Gao, R. Yang, L. Jiang, Biodegradation and mineralization of polystyrene by plastic-eating mealworms: part 1. Chemical and physical characterization and isotopic tests, Environ. Sci. Technol. 49 (2015) 12080–12086, https://doi.org/10.1021/acs.est.5b02661.
[31] S. Jiang, T. Su, J. Zhao, Z. Wang, Biodegradation of polystyrene by *Tenebrio molitor, Galleria mellonella*, and *Zophobas atratus* larvae and comparison of their degradation effects, Polymers 13 (2021) 3539, https://doi.org/10.3390/polym13203539.
[32] L. He, S.-S. Yang, J. Ding, C.-X. Chen, F. Yang, Z.-L. He, J.-W. Pang, B.-Y. Peng, Y. Zhang, D.-F. Xing, N.-Q. Ren, W.-M. Wu, Biodegradation of polyethylene terephthalate by *Tenebrio molitor*: insights for polymer chain size, gut metabolome and host genes, J. Hazard. Mater. 465 (2024) 133446, https://doi.org/10.1016/j.jhazmat.2024.133446.
[33] M.A. Dar, R. Xie, H.M. Zabed, K.D. Pawar, N.P. Dhole, J. Sun, Current paradigms and future challenges in harnessing gut bacterial symbionts of insects for biodegradation of plastic wastes, Insect Sci. 32 (2025) 726–752, https://doi.org/10.1111/1744-7917.13417.
[34] M. Schwarz, G. Tokuda, H. Osaki, A. Mikaelyan, Reevaluating symbiotic digestion in cockroaches: unveiling the hindgut's contribution to digestion in wood-feeding Panesthiinae (Blaberidae), Insects 14 (2023) 768, https://doi.org/10.3390/insects14090768.
[35] J. Sun, A. Prabhu, S.T.N. Aroney, C. Rinke, Insights into plastic biodegradation: community composition and functional capabilities of the superworm (*Zophobas morio*) microbiome in styrofoam feeding trials, Microb. Genom. 8 (2022), https://doi.org/10.1099/mgen.0.000842.
[36] N. Lo, G. Tokuda, H. Watanabe, H. Rose, M. Slaytor, K. Maekawa, C. Bandi, H. Noda, Evidence from multiple gene sequences indicates that termites evolved from wood-feeding cockroaches, Curr. Biol. 10 (2000) 801–804, https://doi.org/10.1016/S0960-9822(00)00561-3.
[37] I. Vital-Vilchis, E. Karunakaran, Using insect larvae and their microbiota for plastic degradation, Insects 16 (2025) 165, https://doi.org/10.3390/insects16020165.
[38] D. Todorović, L. Ilijin, M. Mrdaković, M. Vlahović, A. Filipović, A. Grčić, V. Perić-Mataruga, Long-term exposure of cockroach *Blaptica dubi* a (Insecta: Blaberidae) nymphs to magnetic fields of different characteristics: effects on antioxidant biomarkers and nymphal gut mass, Int. J. Radiat. Biol. 95 (2019) 1185–1193, https://doi.org/10.1080/09553002.2019.1589017.
[39] I.A. Adedara, K.A. Mohammed, O.F. Da-Silva, F.A. Salaudeen, F.L.S. Gonçalves, D.B. Rosemberg, M. Aschner, J.B.T. Rocha, E.O. Farombi, Utility of cockroach as a model organism in the assessment of toxicological impacts of environmental pollutants, Environ. Adv. 8 (2022) 100195, https://doi.org/10.1016/j.envadv.2022.100195.
[40] M.-X. Li, S.-S. Yang, J. Ding, M.-Q. Ding, L. He, D.-F. Xing, C.S. Criddle, M.E. Benbow, N.-Q. Ren, W.-M. Wu, Cockroach *Blaptica dubia* biodegrades polystyrene plastics: nsights for superior ability, microbiome and host genes, J. Hazard. Mater. 479 (2024) 135756, https://doi.org/10.1016/j.jhazmat.2024.135756.
[41] M. Maziarz, Accurate Molecular Weight Determination of polystyrene-tetrahydrofuran Solutions Using the Arc™ HPLC System with a Strong Solvent Compatibility Kit and Refractive Index (RI) Detector, Waters Corporation, 2024.
[42] A.M. Striegel, W.W. Yau, J.J. Kirkland, D.D. Bly, Modern Size-Exclusion Liquid Chromatography: Practice of Gel Permeation and Gel Filtration Chromatography, first ed., Wiley, 2009 https://doi.org/10.1002/9780470442876.
[43] A. Hirokazu, The ABCs of measurement methods: KBr pellet method, FTIR Talk Lett. 14 (2010) 4–6.
[44] D. Chauhan, G. Agrawal, S. Deshmukh, S.S. Roy, R. Priyadarshini, Biofilm formation by *Exiguobacterium* sp. DR11 and DR14 alter polystyrene surface properties and initiate biodegradation, RSC Adv. 8 (2018) 37590–37599, https://doi.org/10.1039/C8RA06448B.
[45] G. Giaganini, M. Cifelli, D. Biagini, S. Ghimenti, A. Corti, V. Castelvetro, V. Domenici, T. Lomonaco, Multi-analytical approach to characterize the degradation of different types of microplastics: identification and quantification of released organic compounds, Molecules 28 (2023) 1382, https://doi.org/10.3390/molecules28031382.
[46] F.-L. Xu, C. Yang, W. He, Q.-S. He, Y.-L. Li, L. Kang, W.-X. Liu, Y.-Q. Xiong, B. Xing, Bias and association of sediment organic matter source apportionment indicators: a case study in a eutrophic Lake Chaohu, China, Sci. Total Environ. 581–582 (2017) 874–884, https://doi.org/10.1016/j.scitotenv.2017.01.037.
[47] C. Westphal, C. Perrot, S. Karlsson, Py-GC/MS as a means to predict degree of degradation by giving microstructural changes modelled on LDPE and PLA, Polym. Degrad. Stabil. 73 (2001) 281–287, https://doi.org/10.1016/S0141-3910(01)00089-1.
[48] S.-S. Yang, W.-M. Wu, A.M. Brandon, H.-Q. Fan, J.P. Receveur, Y. Li, Z.-Y. Wang, R. Fan, R.L. McClellan, S.-H. Gao, D. Ning, D.H. Phillips, B.-Y. Peng, H. Wang, S.-Y. Cai, P. Li, W.-W. Cai, L.-Y. Ding, J. Yang, M. Zheng, J. Ren, Y.-L. Zhang, J. Gao, D. Xing, N.-Q. Ren, R.M. Waymouth, J. Zhou, H.-C. Tao, C.J. Picard, M.E. Benbow, C.S. Criddle, Ubiquity of polystyrene digestion and biodegradation within yellow mealworms, larvae of *Tenebrio molitor* Linnaeus (Coleoptera: Tenebrionidae), Chemosphere 212 (2018) 262–271, https://doi.org/10.1016/j.chemosphere.2018.08.078.
[49] B.-Y. Peng, S. Xiao, Y. Sun, Y. Liu, J. Chen, X. Zhou, W.-M. Wu, Y. Zhang, Unveiling fragmentation of plastic particles during biodegradation of polystyrene and polyethylene foams in mealworms: highly sensitive detection and digestive modeling prediction, Environ. Sci. Technol. 57 (2023) 15099–15111, https://doi.org/10.1021/acs.est.3c04406.
[50] Y. Xu, S. Xiao, Q. Xu, B.-Y. Peng, L. Yang, J. Chen, X. Zhou, W.-M. Wu, Y. Zhang, Responses of $\delta^{13}C$ and reactive oxygen and nitrogen species to microplastics biodegradation in Plastivore mealworms (*Tenebrio molitor*), Chem. Eng. J. 524 (2025) 168859, https://doi.org/10.1016/j.cej.2025.168859.
[51] L. He, J. Ding, S.-S. Yang, Y.-N. Zang, J.-W. Pang, D. Xing, L.-Y. Zhang, N. Ren, W.-M. Wu, Molecular-weight-dependent degradation of plastics: deciphering host–microbiome synergy biodegradation of high-purity polypropylene microplastics by mealworms, Environ. Sci. Technol. 58 (2024) 6647–6658, https://doi.org/10.1021/acs.est.3c06954.
[52] S. Woo, I. Song, H.J. Cha, Fast and facile biodegradation of polystyrene by the gut microbial flora of *Plesiophthalmus davidis* larvae, Appl. Environ. Microbiol. 86 (2020) e01361, https://doi.org/10.1128/AEM.01361-20, 20.
[53] S. Behera, S. Das, Potential and prospects of *Actinobacteria* in the bioremediation of environmental pollutants: cellular mechanisms and genetic regulations, Microbiol. Res. 273 (2023) 127399, https://doi.org/10.1016/j.micres.2023.127399.
[54] W.-H. Li, D.-C. Jin, F.-L. Li, Y. Cheng, J.-X. Jin, Metabolic phenomics of bacterium *Pantoea* sp. from larval gut of the diamondback moth, *Plutella xylostella* (Lepidoptera: Plutellidae), Symbiosis 72 (2017) 135–142, https://doi.org/10.1007/s13199-016-0453-4.
[55] W. Jindachot, C. Treesubsuntorn, P. Thiravetyan, Effect of individual/co-culture of native phyllosphere organisms to enhance *Dracaena sanderiana* for benzene phytoremediation, Water Air Soil Pollut. 229 (2018) 80, https://doi.org/10.1007/s11270-018-3735-z.
[56] H. Saygin, A. Baysal, Insights into the degradation behavior of

submicroplastics by *Klebsiella pneumoniae*, J. Polym. Environ. 29 (2021) 958–966, https://doi.org/10.1007/s10924-020-01929-y.
[57] J. Rajkumari, L.P. Singha, P. Pandey, Draft genome sequence of *Klebsiella pneumoniae* AWD5, Genome Announc. 5 (2017) e01531, https://doi.org/10.1128/genomeA.01531-16, 16.
[58] A.M. Brandon, S.-H. Gao, R. Tian, D. Ning, S.-S. Yang, J. Zhou, W.-M. Wu, C.S. Criddle, Biodegradation of polyethylene and plastic mixtures in mealworms (Larvae of *Tenebrio molitor*) and effects on the gut microbiome, Environ. Sci. Technol. 52 (2018) 6526–6533, https://doi.org/10.1021/acs.est.8b02301.
[59] H.R. Kim, H.M. Lee, H.C. Yu, E. Jeon, S. Lee, J. Li, D.-H. Kim, Biodegradation of polystyrene by *Pseudomonas* sp. isolated from the gut of superworms (larvae of *Zophobas atratus*), Environ. Sci. Technol. 54 (2020) 6987–6996, https://doi.org/10.1021/acs.est.0c01495.
[60] J.T. Osvatic, L.G.E. Wilkins, L. Leibrecht, M. Leray, S. Zauner, J. Polzin, Y. Camacho, O. Gros, J.A. Van Gils, J.A. Eisen, J.M. Petersen, B. Yuen, Global biogeography of chemosynthetic symbionts reveals both localized and globally distributed symbiont groups, Proc. Natl. Acad. Sci. 118 (2021) e2104378118, https://doi.org/10.1073/pnas.2104378118.
[61] E. Mahmoud, A. Hanora, S. Abdalla, A.A. Abdelrahman Ahmed, S. Zakeer, Shotgun metagenomic analysis of bacterial symbionts associated with "Chromodoris quadricolor" mantle, Mar. Genom. 69 (2023) 101030, https://doi.org/10.1016/j.margen.2023.101030.
[62] G. Kwon, J. Lee, Y.-H. Lim, Dairy *Propionibacterium* extends the mean lifespan of *Caenorhabditis elegans* via activation of the innate immune system, Sci. Rep. 6 (2016) 31713, https://doi.org/10.1038/srep31713.
[63] Z. Nie, B. Yan, Y. Xu, M.K. Awasthi, H. Yang, Characterization of pyridine biodegradation by two *Enterobacter* sp. strains immobilized on *Solidago canadensis* L. stem derived biochar, J. Hazard. Mater. 414 (2021) 125577, https://doi.org/10.1016/j.jhazmat.2021.125577.
[64] M. Tavares, M. Kozak, A. Balola, C.P. Coutinho, C.P. Godinho, A.A. Hassan, V.S. Cooper, I. Sá-Correia, Adaptation and survival of *Burkholderia cepacia* and *B. contaminans* during long-term incubation in saline solutions containing benzalkonium chloride, Front. Bioeng. Biotechnol. 8 (2020) 630, https://doi.org/10.3389/fbioe.2020.00630.
[65] B. Tiwari, N. Manickam, S. Kumari, A. Tiwari, Biodegradation and dissolution of polyaromatic hydrocarbons by *Stenotrophomonas* sp, Bioresour. Technol. 216 (2016) 1102–1105, https://doi.org/10.1016/j.biortech.2016.06.047.
[66] H.T. Kwon, E.H. Jang, S.K. Na, A.R. Shin, A.Y. Kim, Y.M. Chi, H. Park, Complete genome sequence of *Stenotrophomonas* sp. KCTC 12332, a biotechnological potential bacterium, J. Biotechnol. 256 (2017) 27–30, https://doi.org/10.1016/j.jbiotec.2017.06.1207.
[67] H.M. Wexler, *Bacteroides* : the Good, the bad, and the nitty-gritty, Clin. Microbiol. Rev. 20 (2007) 593–621, https://doi.org/10.1128/CMR.00008-07.
[68] E. Petit, M.V. Coppi, J.C. Hayes, A.C. Tolonen, T. Warnick, W.G. Latouf, D. Amisano, A. Biddle, S. Mukherjee, N. Ivanova, A. Lykidis, M. Land, L. Hauser, N. Kyrpides, B. Henrissat, J. Lau, D.J. Schnell, G.M. Church, S.B. Leschine, J.L. Blanchard, Genome and transcriptome of clostridium phytofermentans, catalyst for the direct conversion of plant feedstocks to fuels, PLoS One 10 (2015) e0118285, https://doi.org/10.1371/journal.pone.0118285.
[69] E. Devillard, D.B. Goodheart, S.K.R. Karnati, E.A. Bayer, R. Lamed, J. Miron, K.E. Nelson, M. Morrison, *Ruminococcus albus* 8 mutants defective in cellulose degradation are deficient in two processive endocellulases, Cel48A and Cel9B, both of which possess a novel modular architecture, J. Bacteriol. 186 (2004) 136–145, https://doi.org/10.1128/JB.186.1.136-145.2004.
[70] S.A. Howard, R. De Dios, E. Maslova, A. Myridakis, T.H. Miller, R.R. McCarthy, Pseudomonas aeruginosa clinical isolates can encode plastic-degrading enzymes that allow survival on plastic and augment biofilm formation, Cell Rep. 44 (2025) 115650, https://doi.org/10.1016/j.celrep.2025.115650.
[71] S. Jindal, K.K. Aggarwal, Assessment of phenanthrene-degrading potential of *Klebsiella pneumoniae* SJK1 isolated from an oil-contaminated site, Microbiology 92 (2023) 572–586, https://doi.org/10.1134/S0026261722602585.
[72] Z. You, H. Xu, S. Zhang, H. Kim, P.-C. Chiang, W. Yun, L. Zhang, M. He, Comparison of petroleum hydrocarbons degradation by *Klebsiella pneumoniae* and *Pseudomonas aeruginosa*, Appl. Sci. 8 (2018) 2551, https://doi.org/10.3390/app8122551.
[73] P.A. Wani, A.A. Abiodun, Y.K. Olusesi, N. Rafi, U. Wani, O.I. Oluwaseun, A.A.O. Sirajudeen, Hydrocarbon degradation and metal remediation by hydrocarbon-utilising and metal-tolerant *Klebsiella pneumoniae* YSA-9 isolated from soil contaminated with petroleum, Chem. Ecol. 38 (2022) 744–759, https://doi.org/10.1080/02757540.2022.2117308.
[74] H.M. Lee, H.R. Kim, E. Jeon, H.C. Yu, S. Lee, J. Li, D.-H. Kim, Evaluation of the biodegradation efficiency of four various types of plastics by *Pseudomonas aeruginosa* isolated from the gut extract of superworms, Microorganisms 8 (2020) 1341, https://doi.org/10.3390/microorganisms8091341.
[75] Y. Zhang, Y. Lin, H. Gou, X. Feng, X. Zhang, L. Yang, Screening of polyethylene-degrading bacteria from *Rhyzopertha dominica* and evaluation of its key enzymes degrading polyethylene, Polymers 14 (2022) 5127, https://doi.org/10.3390/polym14235127.
[76] M. Bansal, D. Santhiya, J.G. Sharma, Simulated dump yard microbes drive significant biodegradation of polypropylene and polyvinyl chloride microplastics, J. Hazard. Mater. 494 (2025) 138545, https://doi.org/10.1016/j.jhazmat.2025.138545.
[77] J. Jin, Y. Shi, B. Zhang, D. Wan, Q. Zhang, An integrated method for studying the biodegradation of benzo[a]pyrene by *Citrobacter* sp. HJS-1 and interaction mechanism based on the structural model of the initial dioxygenase, Environ. Sci. Pollut. Res. 30 (2023) 85558–85568, https://doi.org/10.1007/s11356-023-28505-w.
[78] J. Hörig, P. Renz, Biosynthesis of vitamin B_{12} formation of free 5,6-dimethylbenzimidazole and α-ribazole from riboflavin by *Propionibacterium freudenreichii*, FEBS Lett. 80 (1977) 337–339, https://doi.org/10.1016/0014-5793(77)80470-5.
[79] S. Skariyachan, V. Manjunatha, S. Sultana, C. Jois, V. Bai, K.S. Vasist, Novel bacterial consortia isolated from plastic garbage processing areas demonstrated enhanced degradation for low density polyethylene, Environ. Sci. Pollut. Res. 23 (2016) 18307–18319, https://doi.org/10.1007/s11356-016-7000-y.
[80] M.-Q. Ding, S.-S. Yang, J. Ding, Z.-R. Zhang, Y.-L. Zhao, W. Dai, H.-J. Sun, L. Zhao, D. Xing, N. Ren, W.-M. Wu, Gut microbiome associating with carbon and nitrogen metabolism during biodegradation of polyethene in *Tenebrio* larvae with crop residues as co-diets, Environ. Sci. Technol. 57 (2023) 3031–3041, https://doi.org/10.1021/acs.est.2c05009.
[81] F. De Filippis, M. Bonelli, D. Bruno, G. Sequino, A. Montali, M. Reguzzoni, E. Pasolli, D. Savy, S. Cangemi, V. Cozzolino, G. Tettamanti, D. Ercolini, M. Casartelli, S. Caccia, Plastics shape the black soldier fly larvae gut microbiome and select for biodegrading functions, Microbiome 11 (2023) 205, https://doi.org/10.1186/s40168-023-01649-0.
[82] T. Mamtimin, H. Han, A. Khan, P. Feng, Q. Zhang, X. Ma, Y. Fang, P. Liu, S. Kulshrestha, T. Shigaki, X. Li, Gut microbiome of mealworms (*Tenebrio molitor* larvae) show similar responses to polystyrene and corn straw diets, Microbiome 11 (2023) 98, https://doi.org/10.1186/s40168-023-01550-w.
[83] Y. Zhu, H. Wang, J. Bai, Y. Qi, D. Han, Biodegradation potential of *Gordonia* spp. on polypropylene and polystyrene: enhanced degradation through pretreatment, Front. Microbiol. 16 (2025) 1621498, https://doi.org/10.3389/fmicb.2025.1621498.
[84] L. Xu, X. An, H. Jiang, R. Pei, Z. Li, J. Wen, W. Pi, Q. Zhang, A novel *Gordonia* sp. PS3 isolated from the gut of *Galleria mellonella* larvae: mechanism of polystyrene biodegradation and environmental toxicological evaluation, J. Hazard. Mater. 488 (2025) 137219, https://doi.org/10.1016/j.jhazmat.2025.137219.
[85] S. Venegas, C. Alarcón, J. Araya, M. Gatica, V. Morin, E. Tarifeño-Saldivia, E. Uribe, Biodegradation of polystyrene by *Galleria mellonella*: identification of potential enzymes involved in the degradative pathway, Int. J. Mol. Sci. 25 (2024) 1576, https://doi.org/10.3390/ijms25031576.
[86] H. Nakatani, Y. Yamaura, Y. Mizuno, S. Motokucho, A.T.N. Dao, H. Nakahara, Biodegradation mechanism of polystyrene by mealworms (*Tenebrio molitor*) and nutrients influencing their growth, Polymers 16 (2024) 1632, https://doi.org/10.3390/polym16121632.
[87] L. Hou, E.L.-W. Majumder, Potential for and distribution of enzymatic biodegradation of polystyrene by environmental microorganisms, Materials 14 (2021) 503, https://doi.org/10.3390/ma14030503.
[88] K.A. Tinker, E.A. Ottesen, The core gut microbiome of the American cockroach, *Periplaneta americana*, is stable and resilient to dietary shifts, Appl. Environ. Microbiol. 82 (2016) 6603–6610, https://doi.org/10.1128/AEM.01837-16.
[89] A.E. Pérez-Cobas, E. Maiques, A. Angelova, P. Carrasco, A. Moya, A. Latorre, Diet shapes the gut microbiota of the omnivorous cockroach *Blattella germanica*, FEMS Microbiol. Ecol. 91 (2015), https://doi.org/10.1093/femsec/fiv022.